2021

Shale wettability: Data sets, challenges, and outlook

Muhammad Arif

Yihuai Zhang

Stefan Iglauer
Edith Cowan University

Shale Wettability: Data Sets, Challenges, and Outlook

Muhammad Arif,* Yihuai Zhang, and Stefan Iglauer

Read Online

ACCESS | Metrics & More | Article Recommendations

ABSTRACT: The wetting characteristics of shale rocks at representative subsurface conditions remain an area of active debate. A precise characterization of shale wettability is essential for enhanced oil and gas recovery, containment security during CO_2 geo-storage, and flow back efficiency during hydraulic fracturing. While several methods were utilized in the literature to evaluate shale wettability (e.g., contact angle measurements, spontaneous imbibition method ,and NMR method), we here review the recently published data sets on shale contact angle measurements. The objectives of this review are to (a) develop a repository of the recent shale wettability data sets using contact angle measurements at high pressure and temperature (HPHT) conditions, (b) explore the factors influencing shale wettability, (c) identify potential limitations associated with contact angle methods, and (d) provide a research outlook for this area. On the basis of the data reviewed here, we conclude the following: (1)

Shale/oil/brine systems demonstrate water-wet to strongly oil-wet wetting behaviors. (2) Shale/CO_2/brine systems are usually weakly water-wet to CO_2-wet. (3) Shale/CH_4/brine systems are weakly water-wet. The key contributing factors that underpin this high shale wettability variability include, but are not limited to, operating pressure and temperature conditions, total organic content (TOC), mineral matter, and thermal maturity conditions. Thus, this review provides a succinct analysis of the shale wettability contact angle data sets and affords an overview of the current state of the art technology and possible future developments in this area to enhance the understanding of shale wettability.
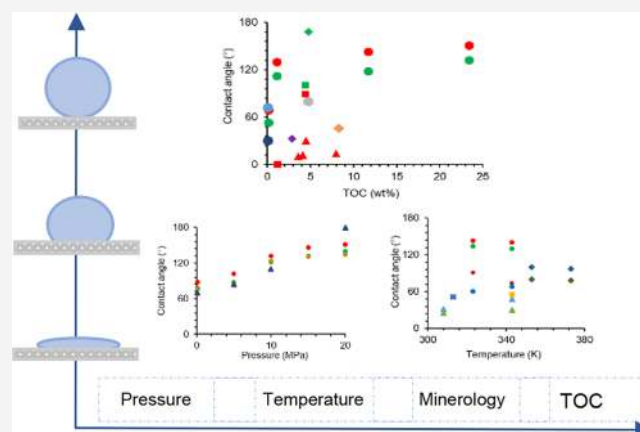
1. INTRODUCTION

Shale rocks have received enormous attention from the global scientific community, especially in the past decade.[1−3] This is arguably due to massive worldwide proven oil and gas reserves in shales.[4] The global technically recoverable reserves (based on technology readiness level and availability) are estimated at 214 trillion m^3 of gas and 419 billion barrels of oil.[5]

Shale oil and gas reservoirs belong to the class of unconventional reservoirs,[6−8] while other unconventional resources include tight oil and gas,[9] coal bed methane,[10−12] and gas hydrates.[13] Shale reservoirs are characterized by an ultralow permeability (order of 10^{-21} m^2 = 1 nano Darcy) and low porosity,[14] and thus, production at economic rates requires advanced technology such as hydraulic fracturing and horizontal drilling.[15] While the "shale revolution" prompted a considerable change in the global energy outlook, the estimates might be widely optimistic,[16] and there are environmental controversies, too.[15] Shales were previously renowned as conventional source rock and caprock. They are now very well established (although poorly understood) as storage media for hydrocarbon accumulations;[17,18] they are also a target for possible CO_2

geo-sequestration and geo-thermal energy production and nuclear waste repositories.[19−24]

From a fundamental perspective, wettability of rock/fluids systems is a physicochemical parameter that governs the fluid distribution and multiphase flow of fluids in a porous medium. Specifically, shale rock wettability is essential due to several aspects. For instance, several enhanced hydrocarbon recovery methods have been proposed and evaluated recently for incremental production from shale reservoirs, e.g., CO_2 flooding in shale oil reservoirs,[25,26] miscible gas injection,[27,28] and CO_2 and N_2 huff-and-puff methods.[29,30] In this context, wettability of shale rock is a key parameter that influences the choice of the appropriate recovery scheme and the associated relative permeability curves for oil−water and oil−gas systems for modeling production from shales. In addition, during CO_2 geo-

storage, the injected CO_2 is rendered immobile by an almost impermeable shale caprock if the shale is water-wet.[31] This structural trapping capacity (of a caprock) is thus a function of shale/CO_2/brine system wettability,[32] and a greater water-wettability of caprock renders structural trapping more efficient. Moreover, shale rocks have recently been evaluated for their potential to act as CO_2 sinks where shale can trap CO_2 by adsorption ("adsorption trapping"). This is attributed to significantly higher CO_2 adsorption capacities than those of methane, as evidenced by several experimental observations[33] and theoretical molecular dynamic predictions.[34] This process thus offers dual benefits, i.e., enhanced methane recovery and simultaneous CO_2 storage.[35,36] Furthermore, spontaneous imbibition of water (which depends on wettability) and thus the water uptake tendency of shales are relevant to the flowback efficiency of fracturing fluid during hydraulic fracturing treatment.[37]

Thus, it is clear that a precise evaluation of shale wettability is extremely important for successful hydrocarbon exploitation from shale reservoirs. Currently, the contact angle method is frequently used to measure shale wettability under different operating conditions,[19,38–40] while spontaneous imbibition has also been extensively studied recently,[41–44] and some NMR investigations have been conducted.[45,46] However, only a few studies have used molecular dynamics simulations to examine shale wettability.[8,47] One key factor that limits the understanding of shale rocks is their complex microstructure,[1,48–52] including organic matter, minerals, and microfractures.[1,53,54] Consequently, a precise shale wettability characterization may not be possible without a detailed understanding of the associated shale microstructure. Furthermore, no single imaging technique is capable to capture the shale rock microstructure fully and accurately, rather a multiscale correlative imaging approach is required.[1,53,54]

The current literature suggests that shale rocks demonstrate a mixed-wet behavior where the inorganic mineral matter is hydrophilic, while the organic matter is hydrophobic,[55] and this hydrophobicity increases with shale total organic carbon (TOC).[19,40] However, there are other observations too where shales were found to be water-wet, and the associated wetting behavior was not influenced by shale TOC,[38] thus suggesting a complex wetting behavior of shales. On the contrary, the wettability of conventional geomaterials, for example, sandstones, and pure minerals are relatively better understood and evaluated.[56–60] For instance, a wide body of literature agrees that pure clean quartz surfaces are strongly water-wet,[61–63] while pure calcite is relatively less water-wet (at ambient conditions), and the water-wetness is typically reduced at elevated CO_2 injection pressures.[32,64–67]

Key factors that influence shale wettability include the TOC, kerogen maturity, and mineral matter.[19,38,39,68] Moreover, contradictions between contact angle and spontaneous imbibition methods (to evaluate shale wettability) were also recently debated. For a review of shale wettability using spontaneous imbibition, the reader is referred to a recent review.[69]

Thus, due to the significance of shale wettability, we here review shale wettability data sets based on the contact angle measurements at high pressure and high temperature conditions. Here, we discuss the impact of pressure, temperature, and TOC for shale/oil/brine systems, shale/CO_2/brine systems, shale/CH_4/brine systems, and shale/CH_4/CO_2/brine systems. Note that a few studies also reported wettability alteration of shales using surfactants;[70,71] however, these data sets are out of scope of this review. This review is intended to act as an entry point for new researchers in this area and to give a state-of-the-art summary of the current understanding of shale wettability.

2. WETTABILITY ASSESSMENT METHODS

Traditionally, wettability of geomaterials (i.e., rocks and minerals) is assessed using a range of methods that include, but are not limited to, contact angle measurements using the sessile drop/captive drop procedure,[56,57,63] spontaneous imbibition method,[72,73] Amott–Harvey and U.S. Bureau of Mines (USBM) methods,[74] capillary rise method,[75] nuclear magnetic resonance (NMR) method,[76] and flotation methods,[77] while relative permeability and capillary pressure curves also provide insights into wettability.[78]

Theoretical molecular dynamic simulations have also been used to characterize wettability of geomaterials by simulating contact angles[79–82] and spontaneous imbibition[83] at a molecular scale.

2.1. Shale Wettability Assessment Methods. There is no single reliable and affordable method for assessing shale wettability, and each method has certain advantages and limitations. The core flooding methods (Amott and USBM tests) to assess shale wettability are notoriously difficult and prone to error (mainly due to the ultralow permeability of the shale and associated long measurement times).

Furthermore, spontaneous imbibition (SI) has been used to determine shale wetting characteristics.[41–43] This method is based on the natural imbibition of water and oil to determine their relative wetting tendencies. The key advantage of SI is that it can assess mixed-wettability behavior of shale surfaces for shale/brine/oil systems,[84] while for a shale/CO_2/brine system forced imbibition may be required which is challenging, especially at high pressure. Wettability characterization using NMR is based on the relative water absorption and oil absorption capacities of brine-saturated and oil-saturated core samples, respectively.[45,46] While NMR spectroscopy is an attractive technique in terms of quantitative evaluation of shale wettability, one key disadvantage is that NMR requires separation of the wetting and nonwetting phase signals and information about the pore size distribution.[76] The contact angle method, which is the focus of this review, is discussed in more detail below.

2.2. Contact Angle Measurement Method. Contact angle measurements are a well-established technique that allows a direct and quantitative assessment of wettability of a given rock/fluid system.[32,57,74,85] In particular, the contact angle method is suitable when pure fluids and clean cores/minerals are used.[86] Another advantage of the contact angle method is that it can provide relatively rapid measurements for a wide spectrum of operating conditions, for example, pressure, temperature, salinity, surface chemistry, and surface roughness of the rock surface. However, caution must be taken during contact angle measurements as surface contamination and surface cleaning methods can lead to a significant bias in reported data.[87] Moreover, contact angle is not a bulk measurement.[88]

The experimental methodology used for contact angle measurements is based on sessile drop or captive bubble configurations; these two approaches are most common in the petroleum industry.[56,86,89] More recently, micromodels are also used for contact angle measurement-associated microscale images; this literally works as a "lab-on-a-chip",[90,91] while X-
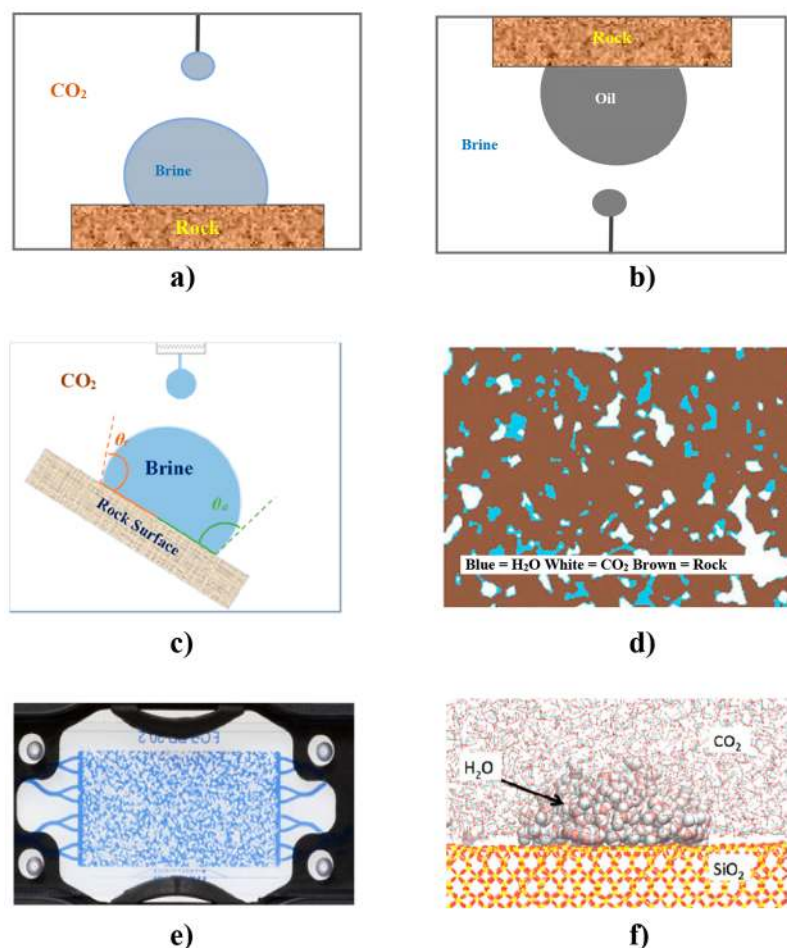
Figure 1. Schematic of different contact angle measurement methods: (a) sessile drop method, (b) captive bubble method, (c) sessile drop tilting plate method, (d) micro-CT imaging method, (e) micromodel method, and (f) molecular dynamic simulation method. Panel (c) is adapted from Arif et al.[56] with permission from Elsevier. Panel (d) is adapted from Iglauer et al.[98] with permission from the American Geophysical Union. Panel (f) is adapted from Iglauer et al.[80] with permission from Elsevier.
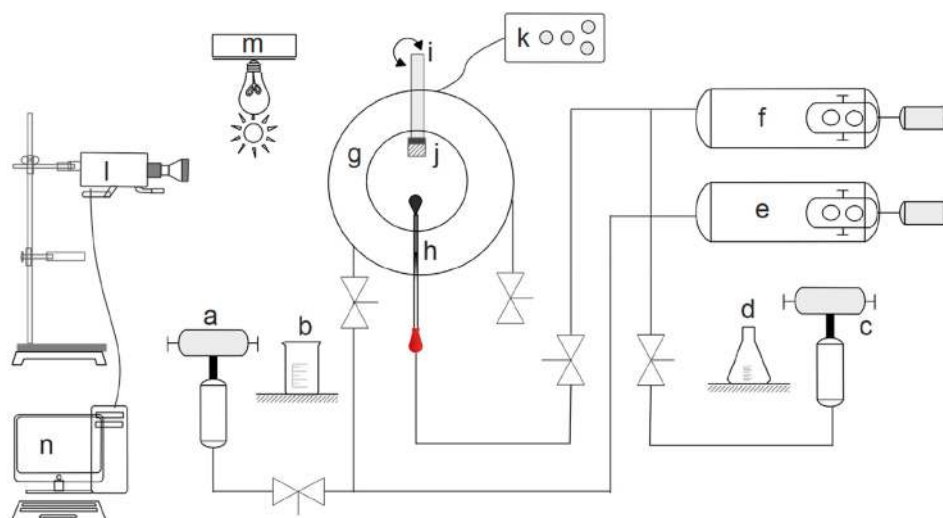
Figure 2. High pressure, high temperature contact angle measurement setup: (a) brine injector, (b) brine feed, (c) crude oil/gas injector, (d) crude oil/gas feed, (e) brine storage, (f) crude oil storage, (g) high pressure, high temperature (HPHT) cell, (h) operating needle, (i) adjustable sample holder, (j) rock sample, (k) pressure and temperature display, (l) video camera, (m) light source, and (n) image visualization software. Adapted from Arif et al.[93] with permission from Elsevier.

ray μ-CT imaging allows real-time localized contact angle measurements at the millimeter scale.[88,92] These methods have the advantage that the fluids reside inside a porous medium; however, experiments are more difficult and costly.

Table 1. Experimental Studies of Contact Angles on Shale Samples at High Pressure and High Temperature Conditions

ref	Sample description	TOC	System considered	Operating conditions	Method	Wetting state[a]
Kaveh et al.[100]	Shaly caprock from North Sea	Not reported	Shale/CO_2/brine	1–14 MPa; 318 K; 1 M NaCl brine	Static contact angles using captive bubble method	Strongly to weakly water-wet
Iglauer et al.[101]	Caprock shale, Australia	0.08%	Shale/CO_2/brine	15 MPa; 323 K	Advancing and receding angles using tilting plate method	Weakly water-wet
Roshan et al.[102]	Perth Basin shale, Australia	0.08%	Shale/air/brine	0.1–20 MPa; 308–243 K	Advancing and receding angles using tilting plate method	Strongly to weakly water-wet
Arif et al.[19]	Three USA shales and Wessex Coast shale, southern England	0.16–23.4 wt %	Shale/CO_2/brine	0.1–20 MPa; 323–343 K	Advancing and receding angles using tilting plate method	Weakly CO_2-wet
Guiltinan et al.[38]	Barnett Shale, USA	3.27–7.88 mass %	Shale/CO_2/brine	up to 13.79 MPa; 293–333 K	X-ray CT scan	Strongly water-wet
Mirchi et al.[70]	Two shale samples	~1–8.3 wt %	Shale/oil/brine	Ambient and 20.6 MPa at 353 K; 0.1–5 M brine	Captive bubble	Strongly water-wet
Qin et al.[103]	Longmaxi Formation, China	3.74%	Shale/CO_2/water	6–18 MPa; 313–353 K; up to 12 days treatment	Sessile drop method	Weakly water-wet to intermediate-wet
Pan et al.[39]	Shengli shale, China	3 wt %	Shale/CO_2/brine; Shale/CH_4/brine	0–20 MPa; 298–343 K	Sessile drop method	Strongly CO_2-wet
Pan et al.[104]	USA and China shales	1.2–20 wt %	Shale/CH_4/brine; Shale/CO_2/n-dodecane	0–25 MPa; 323 K	Sessile drop method	Strongly oil-wet and strongly CO_2-wet
Yekeen et al.[40]	Carbonaceous shale from Malaysia	4.77 wt %	Shale/oil/brine; Shale/CO_2/brine	8–22 MPa; 353–453 K; 0–7 wt %	Captive bubble and sessile drop method	Shale/oil/brine system was oil-wet; shale/CO_2/brine system was CO_2-wet

[a]Wettability is classified as follows: 0° = completely water-wet, 0°–50° = strongly water-wet, 50°–70° = weakly water-wet, 70°–110° = intermediate-wet, 110°–130° = weakly nonwetting, 130°–180° = strongly nonwetting, 180° = completely nonwetting.[32]

Specifically, the captive bubble method (Figure 1) utilizes a flat clean rock sample positioned in a pressure cell. For shale/oil/brine systems, the equipment utilizes two mechanically operated pumps (one for the test fluid to dispense a drop, and another pump for the bulk fluid[93]). The system pressure is gradually increased via mechanical adjustment of the bulk-fluid piston. After stabilization within the brine-filled cell, a droplet of crude oil is dispensed beneath the rock surface via a needle.[86] The droplet forms a contact angle at the three-phase contact line (the intersection of the rock surface and crude oil and brine phases). A similar approach has been utilized to measure contact angles for shale/CO_2/brine systems.[19]

The sessile drop method works in a quasi-opposite way; i.e., a droplet of brine is dispensed in the presence of a gaseous (or oil) environment onto the substrate in the pressure cell. Note that a tilted plate design[19,31,61] allows for the synchronized measurement of water advancing and receding angles.[85] Addition and removal of drop volumes[58] is another way of measuring advancing and receding contact angles. Water advancing contact angles (θ_a) are measured at the leading edge and just before the droplet begins to move and water receding contact angles "θ_r" are measured at the trailing edge of the droplet (where CO_2 is displacing the aqueous phase in a CO_2/brine system). Moreover, the water advancing angle corresponds to the imbibition mechanism, while the water receding angle corresponds to the "drainage", hence the advantage of measuring advancing and receding contact angles over static contact angles.[94] Characteristically, the advancing contact angle is higher than receding contact angles due to "hysteresis", a phenomenon that arises due to surface roughness, chemical or structural heterogeneity, or adsorption/desorption of molecules on "nonideal surfaces".[95−97] Note that if θ_a and θ_r are not measured, and instead only one contact angle is measured on a flat surface, then it is most likely that a metastable drop is

observed (the contact angle then lies anywhere between θ_a and θ_r). Figure 1 shows a schematic illustration of the contact angle measurement method, while Figure 2 shows the high pressure equipment that can measure shale/oil/brine contact angles.

3. REVIEW OF SHALE WETTABILITY DATA

Several data sets were identified where shale wettability was measured at high pressure and temperature conditions (Table 1). While there are several other data sets which reported contact angles of shale at ambient conditions,[99] these were not included in this review, albeit included for a comparison purpose only.

It is clear from Table 1 that shale wettability at high pressure conditions has only been recently investigated, and the data is sparse. It is also evident that the key systems investigated are shale/CO_2/brine systems, shale/oil/brine systems, and shale/CH_4/brine systems.

3.1. Influence of Pressure. The contact angle and thus wettability of shale surfaces are influenced by the injection pressure (or generally the prevailing reservoir pressure). This is particularly true for shale/CO_2/brine systems as evident from Arif et al.'s[19] study, where advancing and receding contact angles for several shales were measured, and a notable impact of pressure on contact angles was found. For instance, when the CO_2 injection pressure was increased from ambient to 10 MPa, θ_a increased from 88° to 132° and θ_r increased from 78° to 123° at a constant temperature of 323 K for a shale sample with 23.4 wt % TOC (Figure 3). These observations suggest that if this shale (TOC = 23.4%) were a caprock during CO_2 storage, the structural trapping capacities of CO_2 will be reduced due to a corresponding reduction in the capillary sealing efficiency of the caprock (for estimation of structural trapping capacities, the reader is referred to Arif et al.[105] and Iglauer[106]). On the
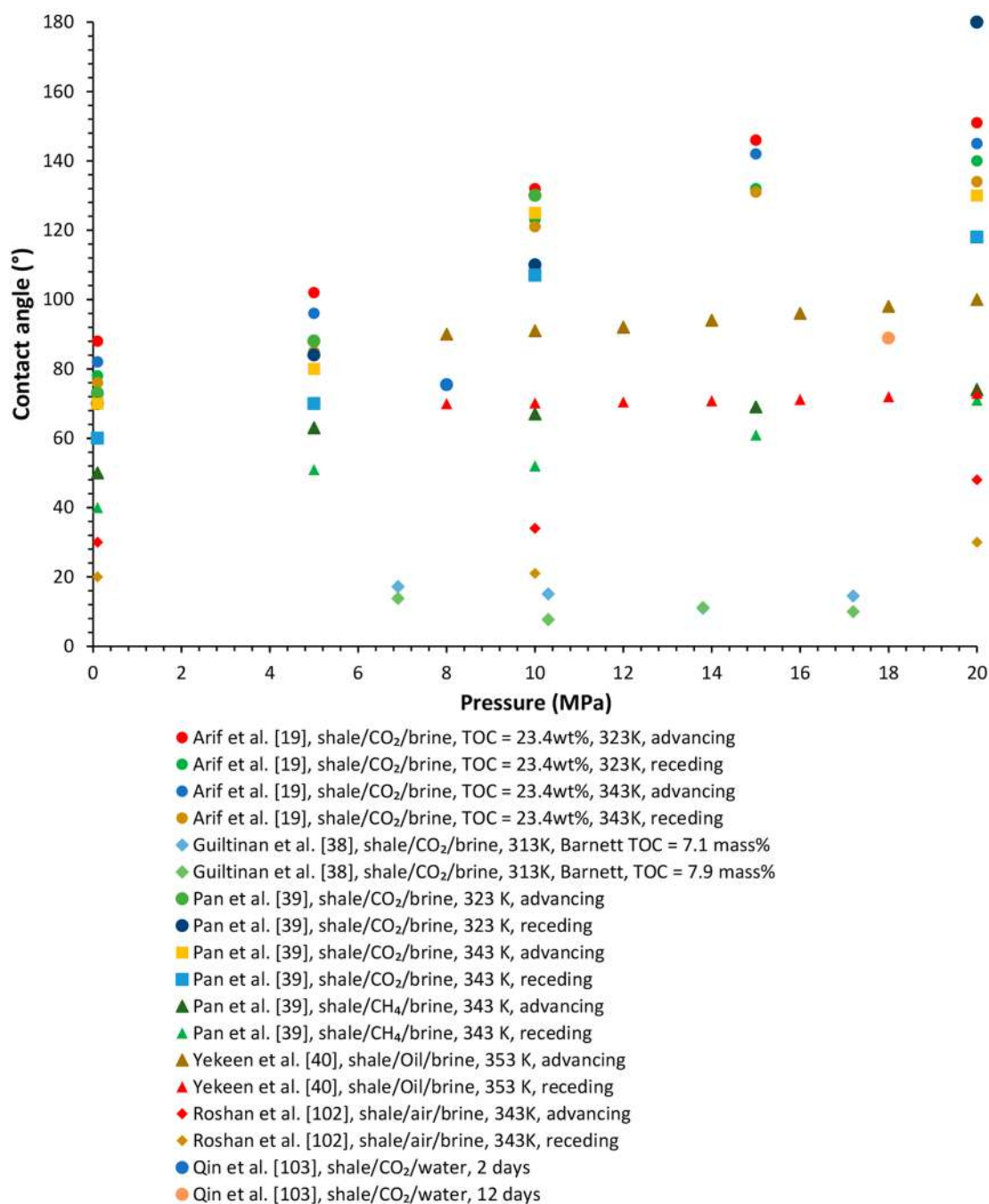
Figure 3. Contact angle (through water) measurements on shale surfaces for various fluid combinations as a function of fluid pressure.

contrary, for CO_2 storage in shale (via adsorption trapping), a higher CO_2 wettability of shale may be more suitable; however, further research is required to confirm this effect.

While Arif et al.'s[19] observations suggested an influence of pressure on shale wettability, Guiltinan et al.'s[38] measurements revealed little or no impact of pressure on contact angles of Barnett Shale samples. Interestingly, here the Barnett Shale samples remained strongly water-wet throughout all test conditions (up to 13.79 MPa;[38] Figure 3). This discrepancy may be due to different surface conditions or types of surface cleaning methods use; note that quartz surfaces cleaned with different cleaning agents demonstrated remarkably different contact angle,[87] although it is still an open question how shales containing organics can be cleaned appropriately (see also

Fauziah et al.[107]). The subsequent data sets for shale/CO_2/brine systems reported by Qin et al.,[103] Pan et al.,[39] and Yekeen et al.[40] demonstrated a clear increase in contact angles with increasing pressure, and overall wettability remained intermediate-wet to weakly CO_2-wet (Figure 3), consistent with Arif et al.[19] Interestingly, Pan et al.[39] found a complete CO_2-wetting state as the observed contact angle reached 180° (Figure 3).

Only a limited amount of studies reported contact angles for shale/air/brine and shale/methane/brine systems as a function of pressure. The contact angles on shale/air brine systems were reported by Roshan et al.,[102] while contact angles for shale/CH_4/brine systems were reported by Pan et al.[39] Notably, the average values of shale/air/brine and shale/methane/brine contact angles are much lower than those for shale/CO_2/brine
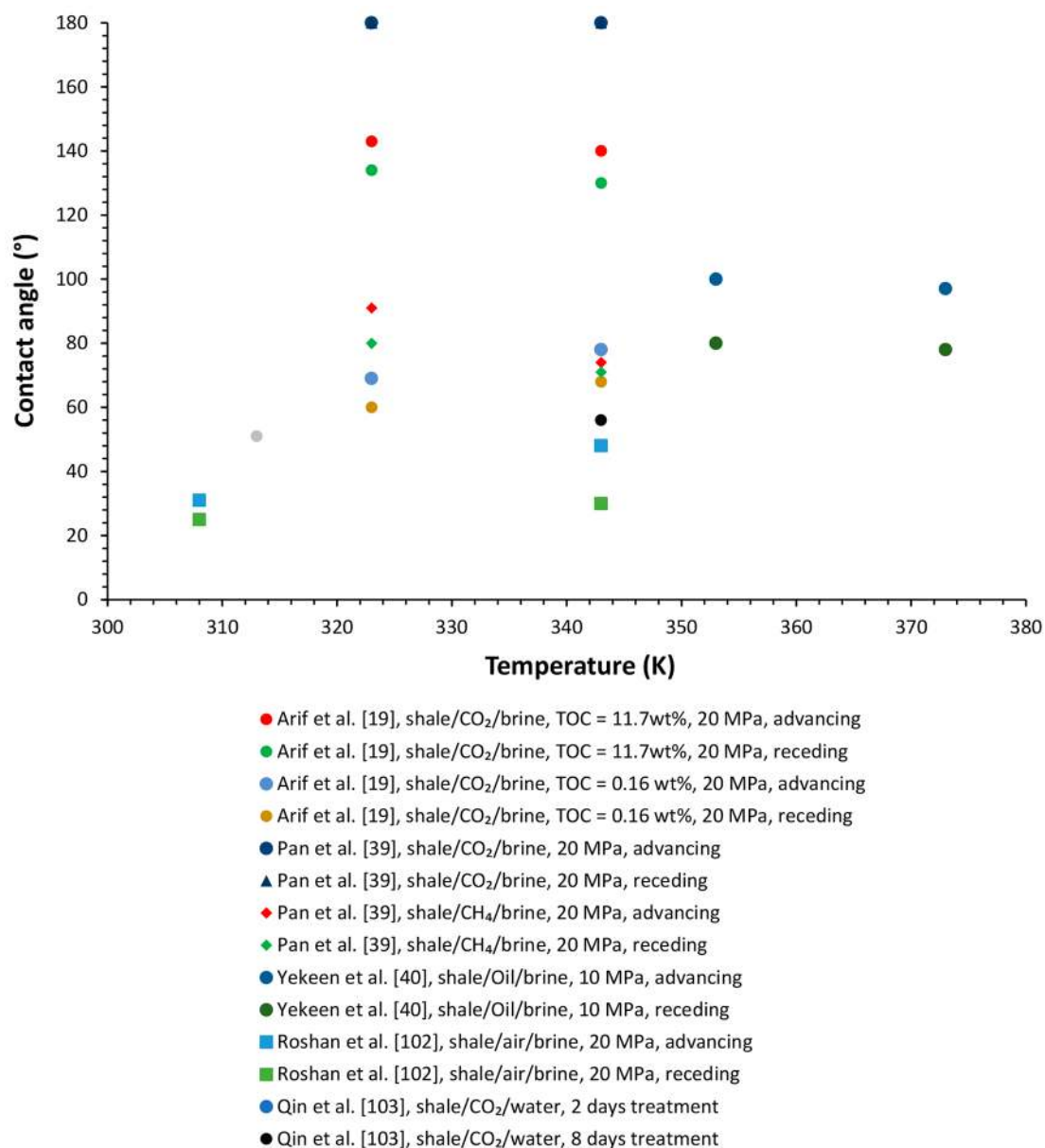
Figure 4. Contact angles (through water) measured on shale surfaces for various fluid combinations as a function of temperature.

(Figure 3). For example, at the same pressure (10 MPa) and temperature (343 K), the receding angles for shale/CO_2/brine, shale/air/brine, and shale/CH_4/brine systems were 122°, 52°, and 21° respectively (Figure 3), suggesting that a shale/CO_2/brine system is the least nonwetting out of the three systems. This can be attributed to the high CO_2 density (CO_2 density at 10 MPa and 343 K = 248 kg/m³),[61,108,109] although TOC also plays a key role (see discussion below).

Note that similar effects have also been observed for pure calcite minerals,[65,67] coal surfaces,[110,111] organic-acid aged calcite surfaces,[112] and mica surfaces[113,105] or quartz.[61]

Furthermore, shale/oil/brine systems, which are relevant to shale oil reservoirs, have only recently been investigated, and the trend indicates an increase in oil-wetness of rocks with increasing pressure.[40] Interestingly, the relative effect of pressure on shale wettability in the presence of oil is much higher than for a comparable carbonate system.[93]

Thus, in summary, there is a consensus that shale tends to lose its water wettability at higher pressures and is relatively more water-wet at lower pressures.

3.2. Influence of Temperature. Wettability of all rock surfaces is influenced by temperature as agreed by classical[74] and recent observations.[93] Thus, shale wettability is also expected to be influenced by changing temperatures. Figure 4 shows the current literature data sets on wettability of shale as a function of temperature.

The data are more limited, and scattering is substantial. It is therefore concluded that the influence of temperature on shale wettability is not well established.

Specifically, Arif et al.[19] reported advancing and receding contact angles for four shale samples (with varying TOC). For medium and high TOC samples, θ_a and θ_r decreased with the increase in temperature; for example, for the shale sample with 11.7 wt % TOC, when the system temperature increased from 323 to 343 K at a fixed pressure 20 MPa, θ_a decreased from 143° to 140°, while θ_r decreased from 134° to 130°, suggesting a small
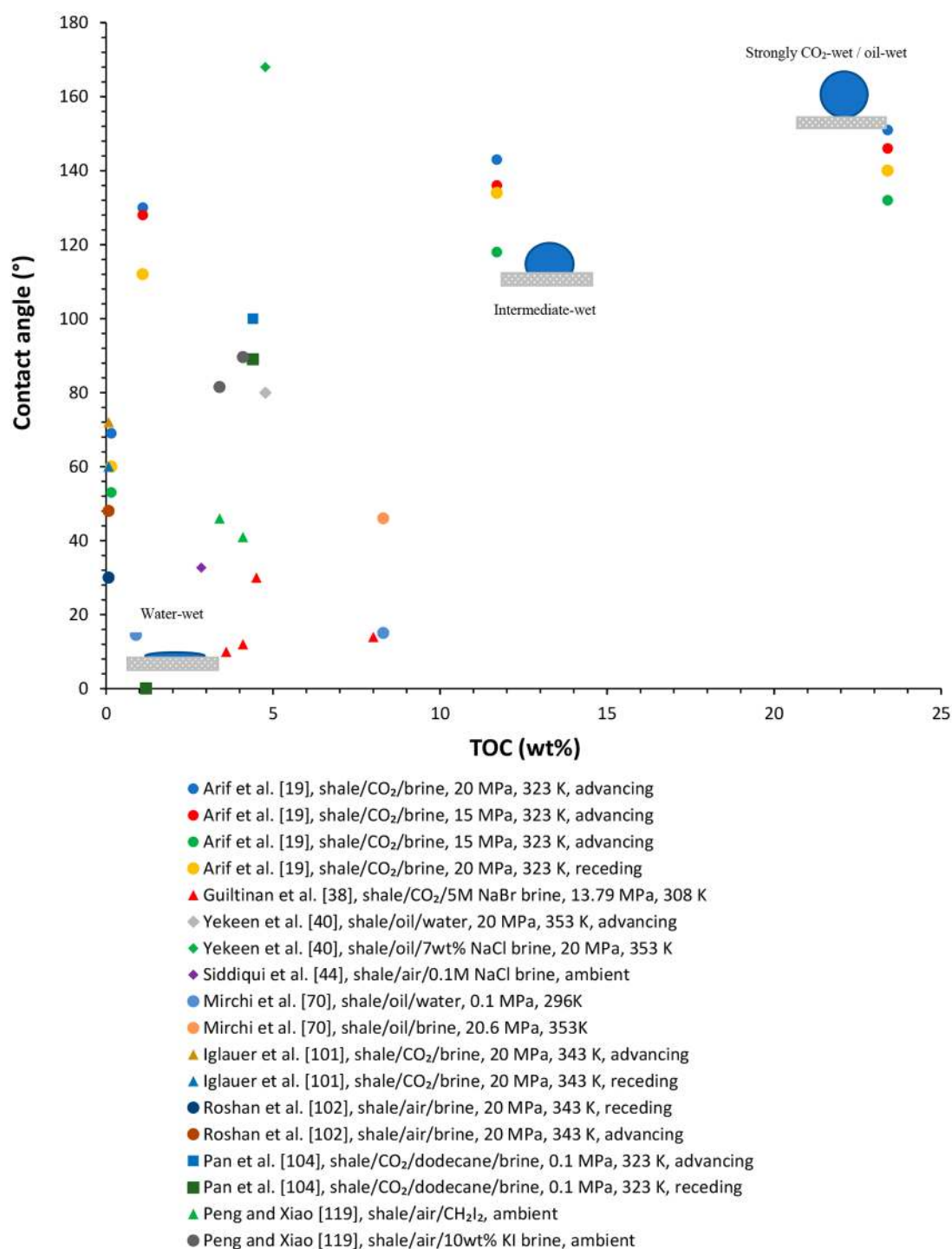
Figure 5. Contact angles (through water) measured on shale surfaces for various fluid combinations as a function of shale TOC.

decrease in CO_2-wettability of the system with increasing temperature. This is consistent with Yekeen et al.'s[40] recent measurements on a Malaysian shale sample (TOC = 4.77 wt %).

Pan et al.[39] analyzed the influence of temperature on shale/CO_2/brine and shale/CH_4/brine contact angles and found that these systems turned more water-wet at elevated temperatures (Figure 4). This decrease in contact angle with temperature may be attributed to a corresponding adjustment in the interfacial energies as depicted by Young's equation.[114]

However, for the shale sample with low TOC (TOC = 0.16 wt %), θ_a and θ_r increased with increasing temperature; for example,

θ_a increased from 69° to 78°, and θ_r increased from 60° to 68°, when the system temperature was elevated from 323 to 343 K (Figure 4).[19] Thus, it appears that temperature increases the water-wettability of medium and high TOC shales, while a low-TOC shale becomes less water-wet with increasing temperature. This agrees with Roshan et al.'s[102] observations where an increase in θ_a and θ_r with increasing temperatures was reported; for example, θ_a increased from 31° to 48° when the system temperature increased from 308 to 343 K (TOC of their sample was 0.08 wt %). However, this area requires further investigations to better understand the fundamental aspects.
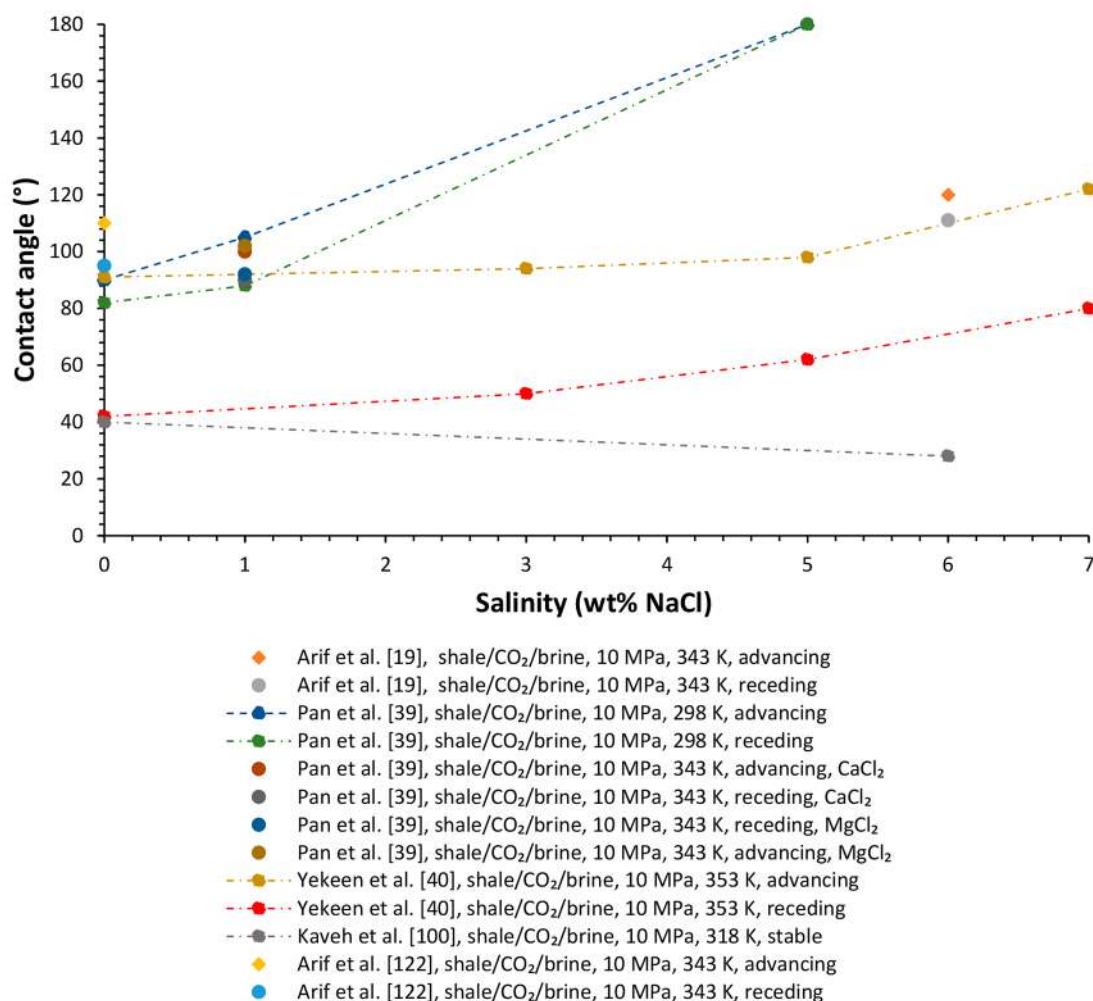
Figure 6. Contact angle on shale surfaces as a function of brine salinity. All data is for NaCl brine unless otherwise stated.

3.3. Influence of Total Organic Content (TOC). The composition and thermal maturity of shale organic matter (kerogen) governs the likelihood of hydrocarbon generation in oil and gas shales.[115] Technically, organic matter can be quantified via chemical measurements or novel machine learning methods,[116] while R_o (vitrinite reflectance) or T_{max} (pyrolysis measurements) are used to determine maturity.[1,54]

Shale wettability is also clearly influenced by its total organic content as suggested by recent experimental studies (Table 1; Figure 5). The shale/CO_2/brine system examined by Arif et al.[19] transitioned from a weakly water-wet state at low TOC (= 0.16 wt %) to a strongly CO_2-wet state at high TOC (= 23.4 wt %) as evidenced by a drastic increase in the water advancing angle from 68° to 151° (Figure 1). This trend was fairly similar at different pressures and temperatures, although the contact angles were generally much lower when the measurements were conducted at lower CO_2 injection pressures. However, there are some contradictory observations, too. For instance, Guiltinan et al.'s[38] X-ray CT observations on the Barnett Shale sample demonstrated no effect of TOC on shale wettability despite TOC varying between 3.27−7.88 wt % (Table 1; Figure 5). Moreover, and interestingly, all Barnett Shale samples remained strongly water-wet, which is consistent with Mirchi et al.'s[70] results, where a shale sample with ∼8 wt % TOC was found to be strongly water-wet (Figure 5). On the contrary, Yekeen et al.'s[40] recent investigation on a shale sample (with TOC = 4.77 wt %)

demonstrated a strongly oil-wet (hydrophobic) behavior ($\theta_a = 168°$), while the low-TOC shale samples analyzed by Iglauer et al.[101] and Roshan et al.[102] demonstrated weakly water-wet behavior.

In terms of wettability, the classical observations of Larter et al.[117] revealed that shales turn intermittently oil-wet due to in situ maturation of organic matter or due to exposure to organic compounds found in formation water. Furthermore, relatively recent investigations confirmed that organic pores tend to be hydrophobic, while inorganic pores are hydrophilic,[118] which is consistent with theoretical molecular dynamics calculations for alkylated versus nonalkylated quartz surfaces[79] (see also discussion in Section 4). Consequently, the composite wetting behavior of shale may be controlled by the connectivity and distribution of organic and inorganic matter.[19,47] Thus, a CO_2-wet high TOC shale may have a a larger fraction of interconnected organic matter pores, while hydrophilic shales appear to have mineral matter as a dominant (surface) phase. However, Peng's and Xiao's[119] observations on Eagle Ford and Barnett Shale samples revealed preferential oil-wet surfaces (oil phase used was diiodomethane (CH_2I_2) and water phase was a 10 wt % KI solution). Notably, however, imbibition measurements (using Micro-CT) by Peng and Xiao[119] showed that water displaced oil from microfractures even in the organic matter layers, indicating water-wet behavior and thus contradicting the contact angle measurements. It was hypothesized

that the formation of a thin water film on the microfracture surface caused the actual contact angle at the microscale to be much smaller.

Another factor that contradicts the theory of "high contact angle for high organic matter content" is that the Barnett Shale sample despite having 90% organic matter pores[120] was found to be water-wet,[38] suggesting that shale wettability may not be controlled by just the fraction of organic matter pores but rather the distribution and connectivity of the organic phase inside the shale.

Other observations also suggest that microstructure and characteristics of organic matter pores may be related to wettability. Thus, Yassin and co-workers[68,121] and Begum et al.[84] analyzed the influence of kerogen matter-hosted pores on shale wettability for a broad range of samples (16 Upper Duvernay and 147 Lower Duvernay shale samples). A cross plot of ϕ_{eff} (effective porosity) and k_{Decay} (permeability) vs TOC was created which demonstrated that ϕ_{eff} generally increased with increasing TOC, suggesting that most pores were located inside the organic matter (OM). Moreover, the samples with higher TOC generally had higher k_{Decay}, suggesting that the pores within OM were relatively well connected. The positive correlations of ϕ_{eff} and k_{Decay} with TOC suggest an abundance of pores within the oil-wet OM, which led to strongly oil-wet characteristics of the shale samples.

In summary, further investigations are required to better understand the influence of shale TOC on its wettability.

3.4. Influence of Salinity. Only a few studies investigated the effect of brine salinity on shale wettability (Figure 6). To elucidate this, Arif and co-workers[19,122] found an increase in contact angle for increasing salinity for shale rocks. For instance, at 10 MPa and 343 K, the measured θ_a for 1 M NaCl (∼6 wt %) brine was 120°, while θ_a for 0 M NaCl (0 wt %) brine was 110°.[19,122] Under the same operating pressure and temperature, θ_r was 111° for shale/CO$_2$/1 M NaCl brine and 95° for shale/CO$_2$/DI-water (Figure 6). Furthermore, Pan et al.[39] also found an increase in contact angle with increasing salinity for shale surfaces (Figure 6). At 10 MPa and 298 K, θ_a for a shale/CO$_2$/brine system increased from 90° to 180° when brine salinity increased from 0 wt % NaCl to 5 wt % NaCl, suggesting a considerable increase in contact angle with increasing ionic strength of brine. Similar trends were reported by Yekeen et al.[40] who found a clear increase in contact angle with salinity; for example, θ_a increased from 90° to 122° when brine salinity increased from 0 wt % NaCl to 7 wt % NaCl at 353 K and 10 MPa (Figure 6). However, the absolute values of contact angles were different in each of the aforementioned studies. This is because the shale samples in each study had different TOC and different mineralogy. The shift in wettability from water-wet to less water-wet (or even CO$_2$-wet) with increasing brine salinity is related to a corresponding change in zeta potential and the associated screening effect of electric double layer at shale/brine interfaces[39,40] (compare also Iglauer[60]). However, Kaveh et al.[100] observed a different trend where contact angles were found to decrease with increasing salinity.

Furthermore, Pan et al.[39] also examined the effect of cation type on contact angles for shale/CO$_2$/brine systems. For instance, at 343 K and 10 MPa, the measured θ_a values for brines comprising 1 wt % NaCl, 1 wt % CaCl$_2$, and 1 wt % MgCl$_2$ were 90°, 100°, and 102°, respectively, indicating that contact angles were highest for MgCl$_2$ brine and lowest for NaCl brine at the same salinity.

3.5. Influence of Shale Minerology. The influence of minerology is more clearly established, and nowadays, quite well understood for pure minerals, for example, calcite,[58,59,67] mica,[31] quartz,[61] and dolomitic carbonate rocks.[93] However, shale is remarkably more complex than pure minerals or conventional rocks. This is partly due to shale rocks exhibiting (a) inorganic nanoporosity caused by the fine dispersion of small-scale (micrometer and nanometer scale) clay and nonclay minerals, (b) organic matter porosity due to heterogeneous kerogen distribution, and (c) fracture porosity due to microfracture networks.[1,118,123] According to Loucks et al.,[123] shale pore sizes are categorized into picopores (<1 nm), nanopores (1 nm to 1 μm), micropores (1 μm to 62.5 1 μm), mesopores (62.5 μm to 4 mm), and macropores (>4 mm). Indeed, a range of average pore sizes are evident from several common shale plays, for example, Bakken Shale (= 5 nm), Monterey Shale (= 10−16 nm), Anadarko Basin shales (≥ 50 nm), and Appalachian Devonian shales (= 7−24 nm).[124]

The key mineral constituents of a shale rock include clay minerals (such as kaolinite, chlorite, illite), quartz, and calcite, while traces of carbonates, pyrite, and feldspars are also found.[1,2] One vital factor that potentially controls the variability in distinct wetting behavior of shale samples (as discussed above, compare Figures 3−6) is the varying mineralogy and its associated surface chemistry. For instance, the high TOC Kimmeridge shale from Wessex Coast, Southern England, was found to be strongly CO$_2$-wet as reported by Arif et al.,[19] while the Barnett Shale was found to be strongly water-wet.[38] The minerology of the Kimmeridge shale is 5%−30% quartz, 5%−20% carbonate, 50%−90% clay minerals + mica, and 5% pyrite, while the Barnett Shale is composed of 45% quartz, 5%−7% feldspar, 15%−25% carbonate, 20%−40% clay minerals, and 5% pyrite.[125] Thus, these differences in minerology may be responsible for the distinct wetting behavior of Kimmeridge shale and Barnett Shale samples under similar operating conditions of pressure and temperature. Notably, however, the TOCs of the Kimmeridge shale and Barnett Shale are also remarkably different (23.4 vs 2−8 wt %; Figure 5).

Clay type and content of a shale sample can also have a significant impact on its wettability;[107,126] typically clay reduced the water-wettability of the systems tested. In a recent review, Siddiqui et al.[99] discussed this effect (effect of clay content on shale wettability), although shale rocks tend be generally more water-wet with increasing clay-content.[127,128] However, meta-analysis on contact angle data did not reveal any statistically significant relation between clay content and the shale surface contact angle.[99]

4. MOLECULAR DYNAMICS STUDIES ON SHALE WETTABILITY

Nanoscale fluid flow and distribution in shale is of key importance for reserve and productivity estimates. To evaluate shale at this scale, molecular dynamics simulations offer a virtual experiment on the rock/fluid interactions by modeling pores of varying surface chemistry and aperture. MD simulations are particularly useful when experimental investigations are challenging, for example, very high pressure and temperatures, use of hazardous materials (e.g., H$_2$S, CH$_4$ etc.), or very small length scales. A typical MD model computes intermolecular interaction using nonbonded interactions, bonding potentials, and force calculations, and such models can predict the behavior of three-phase systems (i.e., rock, brine and CO$_2$) under consideration.[80,129,130]

Table 2. Molecular Dynamic Studies of Contact Angles on Shale

ref	Sample description	TOC	System considered	Operating conditions	Method	Wetting state
Hu et al.[47]	Pure and oxidized graphene surfaces	O/C ratios from 0% to 20%	Shale/octane/water	0.1 MPa; 300 K	MD simulation using GROMACS	Mixed-wet
Yu et al.[131]	Pure and oxidized graphene surface	100% carbon	Shale/CO_2/water; Shale/CO_2/CH_4/water	0–40 MPa; 296–343 K	MD simulation using LAMMPS	Surfaces with lower O/C ratios were more hydrophobic

- - -●- - - Arif et al. [19], shale/CO_2/brine, TOC = 23.4wt%, 323K, advancing, Experimental
- - -●- - - Arif et al. [19], shale/CO_2/brine, TOC = 23.4wt%, 323K, receding, Experimental
- - -●- - - Pan et al. [39], shale/CH_4/brine, 323 K, advancing, Experimental
- - -●- - - Yu et al. [131], CO_2/water/graphene, 323 K, MD
- ● Yu et al. [131], CH_4/water/graphene, 323 K, MD
- ● Yu et al. [131], CO_2-CH_4/water/graphene, 323 K, CH_4 = 50%, MD
- ● Yu et al. [131], CO_2/brine/graphene, 323 K, 1M NaCl, MD
- ● Yu et al. [131], CO_2/brine/graphene, 323 K, 1M $MgCl_2$, MD
- ● Yu et al. [31], CO_2/water/graphene, 298 K, MD
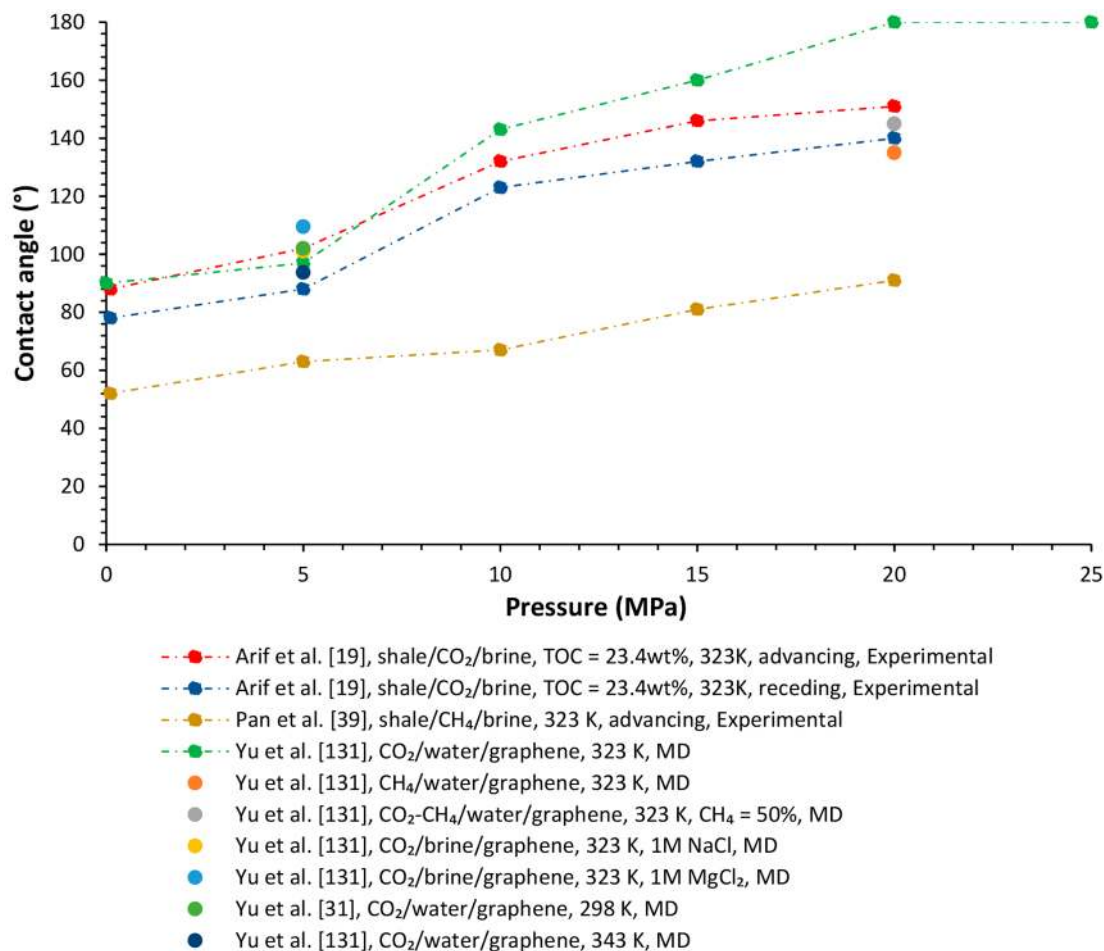- ● Yu et al. [131], CO_2/water/graphene, 343 K, MD

Figure 7. Contact angles (through water) on shale surfaces for various fluid combinations as a function of operating conditions, predicted via molecular dynamics simulations.

However, molecular dynamics simulations for shale/brine systems are currently very limited (Table 2). Note that previous studies have utilized pure and oxidized graphene models to represent an organic pore surface in shales.[47,131,132]

4.1. Effect of Pressure and Temperature on Shale Wettability Predicted via Molecular Dynamics Simulations. There are not many studies on molecular dynamic simulations of shale wettability. However, recently, Yu et al.[131] investigated shale wetting behavior as a function of pressure, temperature, salinity, and CH_4 concentration using graphene as a model surface (Figure 7). Their results indicated a clear increase in contact angle with increasing pressure, consistent with experimental measurements by Arif et al.[19] and Pan et al.[39] The absolute values of contact angles reported by Yu et al.[131] also demonstrated a reasonable consistency with experimental contact angle data (Figure 5). Moreover, the influence of variable CH_4 concentration was also investigated by simulating contact angles for graphene/CO_2/CH_4/brine systems. Such investigations elucidate the wetting behavior pertinent during

CO_2 injection into a shale gas reservoir. At 20 MPa and 323 K, the contact angle for the graphene/CH_4/water system was 135° for pure CH_4, and it increased to 145° at 50% CO_2 and 50% methane concentration (Figure 7). This result suggests that shale gas reservoirs tend to be relatively more CO_2-wet in the presence of CO_2. The increase in contact angle with increasing CO_2 fraction can be attributed a decrease in interfacial tension with increasing CO_2 mole fraction as evident from independent experimental measurements.[133,134] Furthermore, contact angles predicted via molecular dynamics simulations decreased with increasing temperature, thus consistent with most experimental observations (see above). Similarly, the influence of salinity suggested an increase in contact angle with increasing salinity (and cationic charge, consistent with other experimental observations; see Iglauer[60] for a more detailed discussion on this).

4.2. Impact of Thermal Maturity on Shale Wettability. Kerogen is the organic material in shale that provides storage of hydrocarbons in shales by means of adsorption.[34,135] Studies on
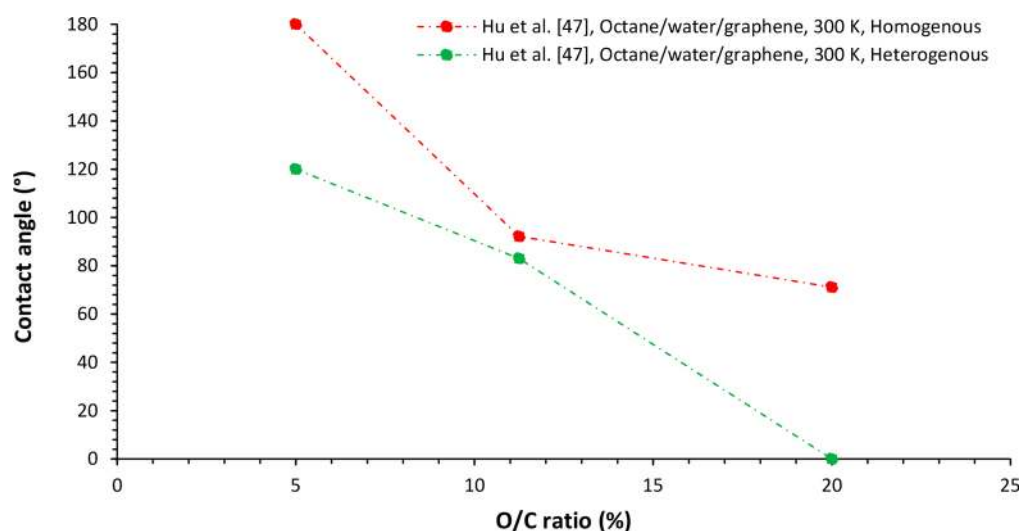
Figure 8. Contact angles (through water) on shale surfaces for various kerogen maturity conditions predicted via molecular dynamics simulations (data from Hu et al.[47]).

shale microstructure via multiscale correlative imaging provide insights into the complex kerogen, distribution, and associated organic matter connectivity.[1,54]

From a geological perspective, heating of kerogen under geothermal pressure and temperature leads to certain changes in the chemical composition of kerogen which in turn leads to different kerogen maturity levels.[136] During kerogen maturation, H/C and O/C ratios tend to decrease due to the loss of hydrocarbons and functionalized molecules.[47] A characteristic van Krevelen diagram, which is a plot of H/C versus O/C ratios, is used to diagnose the thermal maturity and the associated hydrocarbon generation tendency of kerogen.

The level of organic kerogen maturity can have an impact on wettability and thus on the storage of hydrocarbons in organic nanopores.[47] Thus, Hu et al.[47] investigated the wettability of shale/oil/brine systems using a molecular dynamics simulation approach. The shale surfaces were modeled by embedding oxygenated functionalized groups on a graphene surface. The carbonyl (−C=O) group was considered as a representative oxygenated group,[47] and the degree of maturation was quantified by 4-by-4, 6-by-6, and 8-by-8 carbonyl pairs which corresponded to O/C ratios percentages of 5%, 11.25%, and 20%, respectively. Note that the highest O/C ratio represents the least mature shale, while the lowest O/C mol ratio represents highly matured shale.[47] The carbonyl groups were distributed uniformly or randomly on the surface to model homogeneous and heterogeneous kerogen surfaces. The resulting contact angles are shown in Figure 8.

It is clear that with decreasing O/C ratio, contact angles increased; this suggests that with an increase in shale rock maturity, the surface becomes more oil-wetting (hydrophobic). Moreover, at the same maturity level, shale surfaces with heterogeneous distribution of functionalized groups tended to be less oil-wet (Figure 8). Interestingly, for the 20% O/C ratio, the kerogen surfaces turned completely water wetting.[47] This is a remarkable observation, which tends to disagree with the experimental contact angle data (Figure 5). While the experimental contact angle data generally agrees that shale with high organic content is more oil-wet, MD simulations demonstrate that contact angles are also affected by the distribution of organic matter rather than TOC alone.

This shows that higher kerogen heterogeneity (i.e., random distribution of the O/C groups and thus heterogeneous surface activated sites) tends to decrease water contact angles, leading to more water-wet kerogen surfaces.[47] This is consistent with Jagadisan and Heidari,[137] who found that kerogen becomes more oil-wet with increasing maturity; for example, the shale/air/water contact angle increased from 44° to 122° when the O/C ratio decreased from 11% to 7%.

These observations are somewhat comparable to Yang et al.'s[138] study where shale/air/water contact angles were measured as a function of vitrinite reflectance, and it was found that the shales with the highest R_o values (2.2%−3.1%) were most hydrophilic, and those with intermediate R_o values (1.5%−1.58%) were the least hydrophilic. It was concluded that the highly matured shales were relatively less hydrophilic, while overmatured and low maturity shales were water-wet. These observations are to some extent consistent with Yassin et al.[68] who found that the Duvernay Shale samples were oil-wet, and the oil-wetness was associated with a large number of hydrophobic organic nanopores in the organic matter (observed via SEM and MICP data, the diameters of organic nanopores were less than 100 nm).

These observations are slightly consistent with Arif et al.'s[110] observations on coals of various ranks; for example, when vitrinite reflectance of the coal samples increased from 0.35 to 3.9, the water advancing contact angle increased from 116° to 140°, suggesting a decrease in water-wettability with increasing vitrinite reflectance. However, some contradictory observations were found, too. For example, Guiltinan et al.[38] evaluated the impact of thermal maturity on shale wettability, and they used vitrinite reflectance to quantify thermal maturity. It was found that shales with low and high vitrinite reflectance demonstrate the most water-wetting behavior, while those with intermediate vitrinite reflectance exhibited less water-wetting behavior.

Notably the increase in shale hydrophobicity with increasing rock maturity is consistent with spontaneous imbibition measurements, where a general decrease in oil wetting index (WI$_o$) with increasing oxygen index was measured, suggesting that higher kerogen maturity leads to a higher wetting affinity to oil.[84]

Thus, in summary, kerogen maturity and spatial kerogen distribution have a clear impact on wettability, albeit more

experimental work is needed to fully understand the underlying correlations and mechanisms responsible.

5. IMPLICATIONS FOR SHALE WETTABILITY DATA AND CHALLENGES

Shale wettability characterization has direct implications for several key upstream applications including enhanced oil recovery from shale oil rocks and enhanced gas recovery from shale gas formations, CO_2 coupled enhanced oil recovery and geo-storage operations, structural trapping capacity during CO_2 or H_2 geo-storage when shale is a caprock, and water uptake in shales during hydraulic fracturing.

Wetting characteristics of a shale/oil/brine system determine the fluid distributions and associated multiphase flow in a shale oil reservoir. A water-wet shale oil rock may favor the flow of oil owing to an improved relative permeability to oil. Recently, Huang et al.[55] predicted three phase (oil, water, and hydrocarbon gas) relative permeability and the associated multiphase flow and transport behavior in shale using digital rock samples reconstructed from scanned images. The oil production was lower when the shale matrix was uniformly oil-wet (compared to mixed-wet shale). It was pointed out that the difference in oil recovery in mixed-wet and oil-wet shale systems was caused by the inorganic matrix, which is water-wet in mixed-wet shale but oil-wet in oil-wet shale.[55]

Similarly, the wetting behavior of a shale gas reservoir governs the initial fluid distribution of the system while the wettability alteration after CO_2 injection, governed by a shale/CH_4/CO_2/brine system, explains the fluid distribution during CO_2 enhanced methane recovery. The current literature reviewed here, although very limited, indicates an increase in shale CO_2 wettability with increasing injection pressures and CO_2 mole fractions.[131] This can be attributed to a higher adsorption capacity of CO_2 in shales when compared to CH_4 under the same thermophysical conditions as evidenced by experimental observations[139,140] and theoretical predictions.[135,141]

Furthermore, wettability characterization of shale/CO_2/brine systems is relevant to CO_2 geo-storage given that structural trapping capacity is a strong function of wettability of shaly caprock.[32] Several studies agree that a strongly water-wet caprock has a better capillary sealing efficiency and thus prevents the upward migration and leakage of CO_2 through the caprock, while CO_2 may leak through a CO_2-wet caprock.[106] There are a few data sets published in this context, and generally, CO_2-wettability increased with increasing pressure and shale TOC.[19,39,40]

In summary, the key challenges associated with shale wettability characterization identified here include, but are not limited to, influence of operating pressure and temperature conditions, influence of TOC and minerology of shale samples, and organic matter connectivity and distribution. Practically, however, in terms of the reliability of the contact angle method for wettability characterization, caution must be taken during contact angle measurements as contact angles can change significantly with surface contamination, surface cleaning methods, and surface roughness.[56,60,87] It is therefore, due to the serious lack of data, advisable to conduct additional bulk measurements.

6. FUTURE RESEARCH

Despite recent investigations into shale wettability using contact angle measurements, a few aspects for future research are identified and outline as under:

1. Temperature showed contradictory trends, i.e. an increase in contact angle and a decrease in contact angle with increasing temperature were both measured.[19] This effect needs to be further investigated using better theoretical approaches.[56]

2. The complexity of organic matter connectivity and the associated impact on wettability is difficult to quantify with contact angle measurements. Thus, better approaches are required to elucidate this behavior. One possible approach could be comparison between spontaneous imbibition measurements vs contact angles measured.[99]

3. Molecular dynamic simulation data for shale wettability is sparse, and future studies are needed in this area.

4. Shale wettability alteration (due to different wettability alteration agents) has not been investigated much, and such investigations can provide insights into enhanced oil and gas recovery potential from shale rocks.

7. CONCLUSIONS

This review provided an overview and critical analysis of the literature data on shale wettability at high pressure and high temperature conditions. Experimental contact angle data sets were reviewed, and it was found that shale wettability data sets are limited which restricts our understanding of shale wettability. Nevertheless, the following conclusions are drawn from this review:

(1) Shale surfaces tend to dewet with increasing pressure. Also, pressure usually has a pronounced effect on wettability of shale/gas systems, while the associated impact is much lower on shale/oil systems.

(2) There is more consensus on the effect of temperature on shale wettability such that the shale surface becomes more water-wet with increasing temperature; however, some exceptions were found for low TOC shales.

(3) Water wettability of several shale systems was found to decrease with increasing TOC. However, some novel observations suggest that it is not the amount of organic matter, rather it is the OM's connectivity and maturity that impacts wettability.

(4) Shale rocks tend to become more oil-wet with increasing thermal maturity as suggested by experimental observations and molecular dynamics simulations. Indeed, for an O/C ratio of 20% (i.e., immature shale), the kerogen surfaces were found to be completely water wetting.

In summary, further research is required to examine the wettability of shale surfaces at realistic reservoir conditions, and with a particular focus on enhanced oil and gas recovery methods, to successfully exploit these resources.

■ AUTHOR INFORMATION

Corresponding Author

Muhammad Arif − *Department of Petroleum Engineering, Khalifa University, Abu Dhabi 127788, United Arab Emirates;* ⓘ orcid.org/0000-0001-7035-6000; Email: muhammad.arif@ku.ac.ae

Authors

Yihuai Zhang — *Department of Earth Science and Engineering, Imperial College London, London SW7 2BP, United Kingdom*

Stefan Iglauer — *School of Engineering, Petroleum Engineering, Edith Cowan University, 6027 Joondalup, Western Australia, Australia;* ⓘ orcid.org/0000-0002-8080-1590

Complete contact information is available at:
https://pubs.acs.org/10.1021/acs.energyfuels.0c04120

Notes

The authors declare no competing financial interest.

Biographies

Muhammad Arif is an assistant professor in the Petroleum Engineering Department, Khalifa University, United Arab Emirates (UAE). He obtained his Ph.D. in petroleum engineering from Curtin University, Australia. His research interests include enhanced oil recovery, CO_2 geo-storage, surface and interfacial phenomena, and unconventional reservoirs. He is also serving as an associate editor for the *Journal of Petroleum Science and Engineering*, Elsevier.

Yihuai Zhang is a research associate at the Department of Earth Science and Engineering, Imperial College, London. He completed his B.Sc. degree from the China University of Petroleum, Beijing, and Missouri University of Science and Technology, USA, in 2014. He obtained his Ph.D. degree from Curtin University, Australia, in 2018 and then worked as a postdoc at The Lyell Centre, Heriot-Watt University. His research interests include carbon storage, micro-CT imaging, geophysics, and rock mechanics.

Stefan Iglauer is a professor of petroleum engineering at Edith Cowan University, Australia. He received his Ph.D. from Oxford Brookes University in 2002. Afterward, he joined the California Institute of Technology and subsequently Imperial College London as a research fellow. From 2011 to 2018, he was an academic at Curtin University, Australia. His research focuses on nanoenergy applications, CO_2 and hydrogen storage, flow through porous media, general energy production, and climate change mitigation.

■ REFERENCES

(1) Arif, M.; Mahmoud, M.; Zhang, Y.; Iglauer, S. X-ray tomography imaging of shale microstructures: A review in the context of multiscale correlative imaging. *Int. J. Coal Geol.* **2021**, *233*, 103641.

(2) Ross, D. J.; Bustin, R. M. The importance of shale composition and pore structure upon gas storage potential of shale gas reservoirs. *Mar. Pet. Geol.* **2009**, *26* (6), 916−927.

(3) Whitelaw, P.; Uguna, C. N.; Stevens, L. A.; Meredith, W.; Snape, C. E.; Vane, C. H.; Moss-Hayes, V.; Carr, A. D. Shale gas reserve evaluation by laboratory pyrolysis and gas holding capacity consistent with field data. *Nat. Commun.* **2019**, *10* (1), 1−10.

(4) *International Energy Outlook 2017*; U.S. Energy Information Administration, 2017.

(5) *Technically Recoverable Shale Oil and Shale Gas Resources: An Assessment of 137 Shale Formations in 41 Countries Outside the United States*; Independent Statistics & Analysis, U.S. Energy Information Administration, U.S. Department of Energy, Washington, DC, 2013.

(6) Law, B. E.; Curtis, J. Introduction to unconventional petroleum systems. *AAPG Bull.* **2002**, *86* (11), 1851−1852.

(7) Yu, H.; Wang, Z.; Rezaee, R.; Zhang, Y.; Han, T.; Arif, M.; Johnson, L. Porosity estimation in kerogen-bearing shale gas reservoirs. *J. Nat. Gas Sci. Eng.* **2018**, *52*, 575−581.

(8) Yu, H.; Wang, Z.; Wen, F.; Rezaee, C.; Lebedev, M.; Li, X.; Zhang, Y.; Iglauer, S. Reservoir and lithofacies shale classification based on NMR logging. *Petroleum Research* **2020**, *5* (3), 202−209.

(9) Aguilera, R. Flow units: From conventional to tight-gas to shale-gas to tight-oil to shale-oil reservoirs. *SPE Reservoir Eval. Eng.* **2014**, *17* (02), 190−208.

(10) Zhang, Y.; Lebedev, M.; Smith, G.; Jing, Y.; Busch, A.; Iglauer, S. Nano-mechanical properties and pore-scale characterization of different rank coals. *Nat. Resour. Res.* **2020**, *29* (3), 1787−1800.

(11) Zhang, Y.; Lebedev, M.; Jing, Y.; Yu, H.; Iglauer, S. In-situ X-ray micro-computed tomography imaging of the microstructural changes in water-bearing medium rank coal by supercritical CO2 flooding. *Int. J. Coal Geol.* **2019**, *203*, 28−35.

(12) Xu, X.; Wang, Q.; Liu, H.; Zhao, W.; Zhang, Y.; Wang, C. Experimental investigation on the characteristics of transient electromagnetic radiation during the dynamic fracturing progress of gas-bearing coal. *Journal of Geophysics and Engineering* **2020**, *17* (5), 799−812.

(13) Dong, H.; Sun, J.; Arif, M.; Golsanami, N.; Yan, W.; Zhang, Y. A novel hybrid method for gas hydrate filling modes identification via digital rock. *Mar. Pet. Geol.* **2020**, *115*, 104255.

(14) Clarkson, C. R.; Solano, N.; Bustin, R. M.; Bustin, A.; Chalmers, G.; He, L.; Melnichenko, Y. B.; Radliński, A.; Blach, T. P. Pore structure characterization of North American shale gas reservoirs using USANS/SANS, gas adsorption, and mercury intrusion. *Fuel* **2013**, *103*, 606−616.

(15) Howarth, R. W.; Ingraffea, A.; Engelder, T. Should fracking stop? *Nature* **2011**, *477* (7364), 271−275.

(16) Hughes, J. D. A reality check on the shale revolution. *Nature* **2013**, *494* (7437), 307−308.

(17) Aplin, A. C.; Matenaar, I. F.; McCarty, D. K.; van Der Pluijm, B. A. Influence of mechanical compaction and clay mineral diagenesis on the microfabric and pore-scale properties of deep-water Gulf of Mexico mudstones. *Clays Clay Miner.* **2006**, *54* (4), 500−514.

(18) Ma, L.; Slater, T.; Dowey, P. J.; Yue, S.; Rutter, E. H.; Taylor, K. G.; Lee, P. D. Hierarchical integration of porosity in shales. *Sci. Rep.* **2018**, *8* (1), 1−14.

(19) Arif, M.; Lebedev, M.; Barifcani, A.; Iglauer, S. Influence of shale-total organic content on CO2 geo-storage potential. *Geophys. Res. Lett.* **2017**, *44* (17), 8769−8775.

(20) Busch, A.; Alles, S.; Gensterblum, Y.; Prinz, D.; Dewhurst, D. N.; Raven, M. D.; Stanjek, H.; Krooss, B. M. Carbon dioxide storage potential of shales. *Int. J. Greenhouse Gas Control* **2008**, *2* (3), 297−308.

(21) Bossart, P.; Thury, M. Research in the Mont Terri rock laboratory: Quo vadis? *Physics and Chemistry of the Earth, Parts A/B/C* **2007**, *32* (1−7), 19−31.

(22) Dickson, M. H.; Fanelli, M. *Geothermal Energy: Utilization and Technology*; Routledge, 2013.

(23) Kang, S. M.; Fathi, E.; Ambrose, R. J.; Akkutlu, I. Y.; Sigal, R. F. Carbon dioxide storage capacity of organic-rich shales. *SPE J.* **2011**, *16* (04), 842−855.

(24) Mallants, D.; Marivoet, J.; Sillen, X. Performance assessment of the disposal of vitrified high-level waste in a clay layer. *J. Nucl. Mater.* **2001**, *298* (1−2), 125−135.

(25) Fakher, S.; Imqam, A. Application of carbon dioxide injection in shale oil reservoirs for increasing oil recovery and carbon dioxide storage. *Fuel* **2020**, *265*, 116944.

(26) Jin, L.; Sorensen, J. A.; Hawthorne, S. B.; Smith, S. A.; Pekot, L. J.; Bosshart, N. W.; Burton-Kelly, M. E.; Miller, D. J.; Grabanski, C. B.; Gorecki, C. D.; Steadman, E. N.; Harju, J. A. Improving oil recovery by use of carbon dioxide in the Bakken unconventional system: a laboratory investigation. *SPE Reservoir Eval. Eng.* **2017**, *20* (03), 602−612.

(27) Alharthy, N.; Teklu, T. W.; Kazemi, H.; Graves, R. M.; Hawthorne, S. B.; Braunberger, J.; Kurtoglu, B. Enhanced oil recovery in liquid-rich shale reservoirs: laboratory to field. *SPE Reservoir Eval. Eng.* **2018**, *21* (01), 137−159.

(28) Lashgari, H. R.; Sun, A.; Zhang, T.; Pope, G. A.; Lake, L. W. Evaluation of carbon dioxide storage and miscible gas EOR in shale oil reservoirs. *Fuel* **2019**, *241*, 1223−1235.

(29) Jia, B.; Tsau, J.-S.; Barati, R. Role of molecular diffusion in heterogeneous, naturally fractured shale reservoirs during CO2 huff-n-puff. *J. Pet. Sci. Eng.* **2018**, *164*, 31−42.

(30) Nguyen, P.; Carey, J. W.; Viswanathan, H. S.; Porter, M. Effectiveness of supercritical-CO2 and N2 huff-and-puff methods of enhanced oil recovery in shale fracture networks using microfluidic experiments. *Appl. Energy* **2018**, *230*, 160−174.

(31) Arif, M.; Barifcani, A.; Lebedev, M.; Iglauer, S. Structural trapping capacity of oil-wet caprock as a function of pressure, temperature and salinity. *Int. J. Greenhouse Gas Control* **2016**, *50*, 112−120.

(32) Iglauer, S.; Pentland, C.; Busch, A. CO2 wettability of seal and reservoir rocks and the implications for carbon geo-sequestration. *Water Resour. Res.* **2015**, *51* (1), 729−774.

(33) Qin, C.; Jiang, Y.; Luo, Y.; Zhou, J.; Liu, H.; Song, X.; Li, D.; Zhou, F.; Xie, Y. Effect of supercritical CO2 saturation pressures and temperatures on the methane adsorption behaviours of Longmaxi shale. *Energy* **2020**, *206*, 118150.

(34) Zeng, K.; Jiang, P.; Lun, Z.; Xu, R. Molecular simulation of carbon dioxide and methane adsorption in shale organic nanopores. *Energy Fuels* **2019**, *33* (3), 1785−1796.

(35) Godec, M.; Koperna, G.; Petrusak, R.; Oudinot, A. Potential for enhanced gas recovery and CO2 storage in the Marcellus Shale in the Eastern United States. *Int. J. Coal Geol.* **2013**, *118*, 95−104.

(36) Rani, S.; Padmanabhan, E.; Prusty, B. K. Review of gas adsorption in shales for enhanced methane recovery and CO2 storage. *J. Pet. Sci. Eng.* **2019**, *175*, 634−643.

(37) Hussien, O. S.; Elraies, K. A.; Almansour, A.; Husin, H.; Belhaj, A.; Ern, L. Experimental study on the use of surfactant as a fracking fluid additive for improving shale gas productivity. *J. Pet. Sci. Eng.* **2019**, *183*, 106426.

(38) Guiltinan, E. J.; Cardenas, M. B.; Bennett, P. C.; Zhang, T.; Espinoza, D. N. The effect of organic matter and thermal maturity on the wettability of supercritical CO2 on organic shales. *Int. J. Greenhouse Gas Control* **2017**, *65*, 15−22.

(39) Pan, B.; Li, Y.; Wang, H.; Jones, F.; Iglauer, S. CO2 and CH4 wettabilities of organic-rich shale. *Energy Fuels* **2018**, *32* (2), 1914−1922.

(40) Yekeen, N.; Padmanabhan, E.; Abdulelah, H.; Irfan, S. A.; Okunade, O. A.; Khan, J. A.; Negash, B. M. CO2/brine interfacial tension and rock wettability at reservoir conditions: A critical review of previous studies and case study of black shale from Malaysian formation. *J. Pet. Sci. Eng.* **2021**, *196*, 107673.

(41) Gao, Z.; Hu, Q. Pore structure and spontaneous imbibition characteristics of marine and continental shales in China. *AAPG Bull.* **2018**, *102* (10), 1941−1961.

(42) Kibria, M. G.; Hu, Q.; Liu, H.; Zhang, Y.; Kang, J. Pore structure, wettability, and spontaneous imbibition of Woodford shale, Permian Basin, West Texas. *Mar. Pet. Geol.* **2018**, *91*, 735−748.

(43) Roychaudhuri, B.; Tsotsis, T. T.; Jessen, K. An experimental investigation of spontaneous imbibition in gas shales. *J. Pet. Sci. Eng.* **2013**, *111*, 87−97.

(44) Siddiqui, M. A. Q.; Chen, X.; Iglauer, S.; Roshan, H. A multiscale study on shale wettability: Spontaneous imbibition versus contact angle. *Water Resour. Res.* **2019**, *55* (6), 5012−5032.

(45) Odusina, E. O.; Sondergeld, C. H.; Rai, C. S. NMR Study of Shale Wettability. In *Canadian Unconventional Resources Conference*; Society of Petroleum Engineers, Calgary, Alberta, Canada, 2011.

(46) Su, S.; Jiang, Z.; Shan, X.; Zhu, Y.; Wang, P.; Luo, X.; Li, Z.; Zhu, R.; Wang, X. The wettability of shale by NMR measurements and its controlling factors. *J. Pet. Sci. Eng.* **2018**, *169*, 309−316.

(47) Hu, Y.; Devegowda, D.; Sigal, R. A microscopic characterization of wettability in shale kerogen with varying maturity levels. *J. Nat. Gas Sci. Eng.* **2016**, *33*, 1078−1086.

(48) Aljamaan, H.; Ross, C. M.; Kovscek, A. R. Multiscale imaging of gas storage in shales. *SPE J.* **2017**, *22* (06), 1760−1777.

(49) Kelly, S.; El-Sobky, H.; Torres-Verdín, C.; Balhoff, M. T. Assessing the utility of FIB-SEM images for shale digital rock physics. *Adv. Water Resour.* **2016**, *95*, 302−316.

(50) Su, Y.; Zha, M.; Ding, X.; Qu, J.; Gao, C.; Jin, J.; Iglauer, S. Petrographic, palynologic and geochemical characteristics of source rocks of the Permian Lucaogou formation in Jimsar Sag, Junggar Basin, NW China: Origin of organic matter input and depositional environments. *J. Pet. Sci. Eng.* **2019**, *183*, 106364.

(51) Su, Y.; Zha, M.; Ding, X.; Qu, J.; Wang, X.; Yang, C.; Iglauer, S. Pore type and pore size distribution of tight reservoirs in the Permian Lucaogou Formation of the Jimsar Sag, Junggar Basin, NW China. *Mar. Pet. Geol.* **2018**, *89*, 761−774.

(52) Yu, H.; Zhang, Y.; Lebedev, M.; Wang, Z.; Li, X.; Squelch, A.; Verrall, M.; Iglauer, S. X-ray micro-computed tomography and ultrasonic velocity analysis of fractured shale as a function of effective stress. *Mar. Pet. Geol.* **2019**, *110*, 472−482.

(53) Goral, J.; Andrew, M.; Olson, T.; Deo, M. Correlative core-to-pore-scale imaging of shales. *Mar. Pet. Geol.* **2020**, *111*, 886−904.

(54) Ma, L.; Fauchille, A.-L.; Dowey, P. J.; Pilz, F. F.; Courtois, L.; Taylor, K. G.; Lee, P. D. Correlative multi-scale imaging of shales: a review and future perspectives. *Geol. Soc. Spec. Publ.* **2017**, *454* (1), 175−199.

(55) Huang, J.; Jin, T.; Chai, Z.; Barrufet, M.; Killough, J. Compositional simulation of three-phase flow in mixed-wet shale oil reservoir. *Fuel* **2020**, *260*, 116361.

(56) Arif, M.; Abu-Khamsin, S. A.; Iglauer, S. Wettability of rock/CO2/brine and rock/oil/CO2-enriched-brine systems: Critical parametric analysis and future outlook. *Adv. Colloid Interface Sci.* **2019**, *268*, 91−113.

(57) Broseta, D.; Tonnet, N.; Shah, V. Are rocks still water-wet in the presence of dense CO2 or H2S? *Geofluids* **2012**, *12* (4), 280−294.

(58) Chiquet, P.; Daridon, J.-L.; Broseta, D.; Thibeau, S. CO2/water interfacial tensions under pressure and temperature conditions of CO2 geological storage. *Energy Convers. Manage.* **2007**, *48* (3), 736−744.

(59) Espinoza, D. N.; Santamarina, J. C. Water-CO$_2$-mineral systems: Interfacial tension, contact angle, and diffusion—Implications to CO$_2$ geological storage. *Water Resour. Res.* **2010**, *46* (7), na.

(60) Iglauer, S. CO2−water−rock wettability: variability, influencing factors, and implications for CO2 geostorage. *Acc. Chem. Res.* **2017**, *50* (5), 1134−1142.

(61) Al-Yaseri, A. Z.; Roshan, H.; Lebedev, M.; Barifcani, A.; Iglauer, S. Dependence of quartz wettability on fluid density. *Geophys. Res. Lett.* **2016**, *43* (8), 3771−3776.

(62) Botto, J.; Fuchs, S. J.; Fouke, B. W.; Clarens, A. F.; Freiburg, J. T.; Berger, P. M.; Werth, C. J. Effects of mineral surface properties on supercritical CO2 wettability in a siliciclastic reservoir. *Energy Fuels* **2017**, *31* (5), 5275−5285.

(63) Mutailipu, M.; Liu, Y.; Jiang, L.; Zhang, Y. Measurement and estimation of CO2−brine interfacial tension and rock wettability under CO2 sub-and super-critical conditions. *J. Colloid Interface Sci.* **2019**, *534*, 605−617.

(64) Al-Anssari, S.; Arif, M.; Wang, S.; Barifcani, A.; Lebedev, M.; Iglauer, S. Wettability of nano-treated calcite/CO2/brine systems: Implication for enhanced CO2 storage potential. *Int. J. Greenhouse Gas Control* **2017**, *66*, 97−105.

(65) Arif, M.; Lebedev, M.; Barifcani, A.; Iglauer, S. CO2 storage in carbonates: Wettability of calcite. *Int. J. Greenhouse Gas Control* **2017**, *62*, 113−121.

(66) Iglauer, S.; Paluszny, A.; Rahman, T.; Zhang, Y.; Wülling, W.; Lebedev, M. Residual trapping of CO2 in an oil-filled, oil-wet sandstone core: Results of three-phase pore-scale imaging. *Geophys. Res. Lett.* **2019**, *46* (20), 11146−11154.

(67) Stevar, M. S.; Böhm, C.; Notarki, K. T.; Trusler, J. M. Wettability of calcite under carbon storage conditions. *Int. J. Greenhouse Gas Control* **2019**, *84*, 180−189.

(68) Yassin, M. R.; Begum, M.; Dehghanpour, H. Organic shale wettability and its relationship to other petrophysical properties: A Duvernay case study. *Int. J. Coal Geol.* **2017**, *169*, 74−91.

(69) Gao, Z.; Fan, Y.; Hu, Q.; Jiang, Z.; Cheng, Y.; Xuan, Q. A review of shale wettability characterization using spontaneous imbibition experiments. *Mar. Pet. Geol.* **2019**, *109*, 330−338.

(70) Mirchi, V.; Saraji, S.; Goual, L.; Piri, M. Dynamic interfacial tension and wettability of shale in the presence of surfactants at reservoir conditions. *Fuel* **2015**, *148*, 127−138.

(71) Yue, Y.; Chen, S.; Wang, Z.; Yang, X.; Peng, Y.; Cai, J.; Nasr-El-Din, H. A. Improving wellbore stability of shale by adjusting its wettability. *J. Pet. Sci. Eng.* **2018**, *161*, 692−702.

(72) Gao, Z.; Hu, Q. Wettability of Mississippian Barnett Shale samples at different depths: Investigations from directional spontaneous imbibition. *AAPG Bull.* **2016**, *100* (1), 101−114.

(73) Ma, S.; Zhang, X.; Morrow, N.; Zhou, X. Characterization of wettability from spontaneous imbibition measurements. *Journal of Canadian Petroleum Technology* **1999**, *38* (13), na.

(74) Anderson, W. Wettability literature survey-part 2: Wettability measurement. *JPT, J. Pet. Technol.* **1986**, *38* (11), 1246.

(75) Galet, L.; Patry, S.; Dodds, J. Determination of the wettability of powders by the Washburn capillary rise method with bed preparation by a centrifugal packing technique. *J. Colloid Interface Sci.* **2010**, *346* (2), 470−475.

(76) Valori, A.; Hursan, G.; Ma, S. M. Laboratory and downhole wettability from NMR T_1/T_2 ratio. *Petrophysics* **2017**, *58* (04), 352−365.

(77) Sohal, M. A.; Thyne, G.; Søgaard, E. G. Novel application of the flotation technique to measure the wettability changes by ionically modified water for improved oil recovery in carbonates. *Energy Fuels* **2016**, *30* (8), 6306−6320.

(78) Masalmeh, S. K. The effect of wettability heterogeneity on capillary pressure and relative permeability. *J. Pet. Sci. Eng.* **2003**, *39* (3−4), 399−408.

(79) Abramov, A.; Keshavarz, A.; Iglauer, S. Wettability of Fully Hydroxylated and Alkylated (001) α-Quartz Surface in Carbon Dioxide Atmosphere. *J. Phys. Chem. C* **2019**, *123* (14), 9027−9040.

(80) Iglauer, S.; Mathew, M.; Bresme, F. Molecular dynamics computations of brine−CO2 interfacial tensions and brine−CO2−quartz contact angles and their effects on structural and residual trapping mechanisms in carbon geo-sequestration. *J. Colloid Interface Sci.* **2012**, *386* (1), 405−414.

(81) Silvestri, A.; Ataman, E.; Budi, A.; Stipp, S.; Gale, J. D.; Raiteri, P. Wetting Properties of the CO2−Water−Calcite System via Molecular Simulations: Shape and Size Effects. *Langmuir* **2019**, *35* (50), 16669−16678.

(82) Sun, E. W.-H.; Bourg, I. C. Molecular Dynamics Simulations of Mineral Surface Wettability by Water Versus CO2: Thin Films, Contact Angles, and Capillary Pressure in a Silica Nanopore. *J. Phys. Chem. C* **2020**, *124* (46), 25382−25395.

(83) Stukan, M. R.; Ligneul, P.; Crawshaw, J. P.; Boek, E. S. Spontaneous imbibition in nanopores of different roughness and wettability. *Langmuir* **2010**, *26* (16), 13342−13352.

(84) Begum, M.; Yassin, M. R.; Dehghanpour, H. Effect of kerogen maturity on organic shale wettability: A Duvernay case study. *Mar. Pet. Geol.* **2019**, *110*, 483−496.

(85) Lander, L. M.; Siewierski, L. M.; Brittain, W. J.; Vogler, E. A. A systematic comparison of contact angle methods. *Langmuir* **1993**, *9* (8), 2237−2239.

(86) Kaveh, N. S.; Wolf, K.; Ashrafizadeh, S.; Rudolph, E. Effect of coal petrology and pressure on wetting properties of wet coal for CO2 and flue gas storage. *Int. J. Greenhouse Gas Control* **2012**, *11*, S91−S101.

(87) Iglauer, S.; Salamah, A.; Sarmadivaleh, M.; Liu, K.; Phan, C. Contamination of silica surfaces: Impact on water−CO2−quartz and glass contact angle measurements. *Int. J. Greenhouse Gas Control* **2014**, *22*, 325−328.

(88) Tanino, Y.; Ibekwe, A.; Pokrajac, D. Impact of grain roughness on residual nonwetting phase cluster size distribution in packed columns of uniform spheres. *Phys. Rev. E: Stat. Phys., Plasmas, Fluids, Relat. Interdiscip. Top.* **2020**, *102* (1), 013109.

(89) Anderson, W. G. Wettability literature survey-part 1: rock/oil/brine interactions and the effects of core handling on wettability. *JPT, J. Pet. Technol.* **1986**, *38* (10), 1125−1144.

(90) Al-Shajalee, F.; Arif, M.; Machale, J.; Verrall, M.; Almobarak, M.; Iglauer, S.; Wood, C. A Multiscale Investigation of Cross-Linked Polymer Gel Injection in Sandstone Gas Reservoirs: Implications for Water Shutoff Treatment. *Energy Fuels* **2020**, *34* (11), 14046−14057.

(91) Morais, S.; Liu, N.; Diouf, A.; Bernard, D.; Lecoutre, C.; Garrabos, Y.; Marre, S. Monitoring CO2 invasion processes at the pore scale using geological labs on chip. *Lab Chip* **2016**, *16* (18), 3493−3502.

(92) Lv, P.; Liu, Y.; Wang, Z.; Liu, S.; Jiang, L.; Chen, J.; Song, Y. In situ local contact angle measurement in a CO2−brine−sand system using microfocused X-ray CT. *Langmuir* **2017**, *33* (14), 3358−3366.

(93) Arif, M.; Abu-Khamsin, S. A.; Zhang, Y.; Iglauer, S. Experimental investigation of carbonate wettability as a function of mineralogical and thermo-physical conditions. *Fuel* **2020**, *264*, 116846.

(94) Marmur, A.; Della Volpe, C.; Siboni, S.; Amirfazli, A.; Drelich, J. W. Contact angles and wettability: towards common and accurate terminology. *Surf. Innovations* **2017**, *5* (1), 3−8.

(95) Carré, A.; Gastel, J.-C.; Shanahan, M. E. Viscoelastic effects in the spreading of liquids. *Nature* **1996**, *379* (6564), 432−434.

(96) Eral, H. B.; 't Mannetje, D. J. C. M.; Oh, J. M. Contact angle hysteresis: a review of fundamentals and applications. *Colloid Polym. Sci.* **2013**, *291* (2), 247−260.

(97) Neumann, A.; Good, R. Thermodynamics of contact angles. I. Heterogeneous solid surfaces. *J. Colloid Interface Sci.* **1972**, *38* (2), 341−358.

(98) Iglauer, S.; Paluszny, A.; Pentland, C. H.; Blunt, M. J. Residual CO2 imaged with X-ray micro-tomography. *Geophys. Res. Lett.* **2011**, *38* (21), na.

(99) Siddiqui, M. A. Q.; Ali, S.; Fei, H.; Roshan, H. Current understanding of shale wettability: A review on contact angle measurements. *Earth-Sci. Rev.* **2018**, *181*, 1−11.

(100) Kaveh, N. S.; Barnhoorn, A.; Wolf, K.-H. Wettability evaluation of silty shale caprocks for CO2 storage. *Int. J. Greenhouse Gas Control* **2016**, *49*, 425−435.

(101) Iglauer, S.; Al-Yaseri, A. Z.; Rezaee, R.; Lebedev, M. CO2 wettability of caprocks: Implications for structural storage capacity and containment security. *Geophys. Res. Lett.* **2015**, *42* (21), 9279−9284.

(102) Roshan, H.; Al-Yaseri, A.; Sarmadivaleh, M.; Iglauer, S. On wettability of shale rocks. *J. Colloid Interface Sci.* **2016**, *475*, 104−111.

(103) Qin, C.; Jiang, Y.; Luo, Y.; Xian, X.; Liu, H.; Li, Y. Effect of supercritical carbon dioxide treatment time, pressure, and temperature on shale water wettability. *Energy Fuels* **2017**, *31* (1), 493−503.

(104) Pan, B.; Li, Y.; Zhang, M.; Wang, X.; Iglauer, S. Effect of total organic carbon (TOC) content on shale wettability at high pressure and high temperature conditions. *J. Pet. Sci. Eng.* **2020**, *193*, 107374.

(105) Arif, M.; Al-Yaseri, A. Z.; Barifcani, A.; Lebedev, M.; Iglauer, S. Impact of pressure and temperature on CO2−brine−mica contact angles and CO2−brine interfacial tension: Implications for carbon geo-sequestration. *J. Colloid Interface Sci.* **2016**, *462*, 208−215.

(106) Iglauer, S. Optimum storage depths for structural CO2 trapping. *Int. J. Greenhouse Gas Control* **2018**, *77*, 82−87.

(107) Fauziah, C. A.; Al-Yaseri, A. Z.; Jha, N. K.; Lagat, C.; Roshan, H.; Barifcani, A.; Iglauer, S. Carbon dioxide wettability of South West Hub sandstone, Western Australia: Implications for carbon geo-storage. *Int. J. Greenhouse Gas Control* **2020**, *98*, 103064.

(108) Span, R.; Wagner, W. A new equation of state for carbon dioxide covering the fluid region from the triple-point temperature to 1100 K at pressures up to 800 MPa. *J. Phys. Chem. Ref. Data* **1996**, *25* (6), 1509−1596.

(109) Pan, B.; Li, Y.; Xie, L.; Wang, X.; He, Q.; Li, Y.; Hejazi, S. H.; Iglauer, S. Role of fluid density on quartz wettability. *J. Pet. Sci. Eng.* **2019**, *172*, 511−516.

(110) Arif, M.; Barifcani, A.; Lebedev, M.; Iglauer, S. CO2-wettability of low to high rank coal seams: Implications for carbon sequestration and enhanced methane recovery. *Fuel* **2016**, *181*, 680−689.

(111) Ibrahim, A. F.; Nasr-El-Din, H. A. Effect of water salinity on coal wettability during CO2 sequestration in coal seams. *Energy Fuels* **2016**, *30* (9), 7532−7542.

(112) Ali, M.; Al-Anssari, S.; Arif, M.; Barifcani, A.; Sarmadivaleh, M.; Stalker, L.; Lebedev, M.; Iglauer, S. Organic acid concentration thresholds for ageing of carbonate minerals: Implications for CO2 trapping/storage. *J. Colloid Interface Sci.* **2019**, *534*, 88−94.

(113) Ali, M.; Aftab, A.; Arain, Z.-U.-A.; Al-Yaseri, A.; Roshan, H.; Saeedi, A.; Iglauer, S.; Sarmadivaleh, M. Influence of Organic Acid Concentration on Wettability Alteration of Cap-Rock: Implications for CO2 Trapping/Storage. *ACS Appl. Mater. Interfaces* **2020**, *12* (35), 39850−39858.

(114) Arif, M.; Barifcani, A.; Iglauer, S. Solid/CO2 and solid/water interfacial tensions as a function of pressure, temperature, salinity and mineral type: Implications for CO2-wettability and CO2 geo-storage. *Int. J. Greenhouse Gas Control* **2016**, *53*, 263−273.

(115) Bernard, S.; Horsfield, B. Thermal maturation of gas shale systems. *Annu. Rev. Earth Planet. Sci.* **2014**, *42*, 635−651.

(116) Yu, H.; Rezaee, R.; Wang, Z.; Han, T.; Zhang, Y.; Arif, M.; Johnson, L. A new method for TOC estimation in tight shale gas reservoirs. *Int. J. Coal Geol.* **2017**, *179*, 269−277.

(117) Larter, S. R.; Bowler, B. F. J.; Li, M.; Chen, M.; Brincat, D.; Bennett, B.; Noke, K.; Donohoe, P.; Simmons, D.; Kohnen, M.; Allan, J.; Telnaes, N.; Horstad, I. Molecular indicators of secondary oil migration distances. *Nature* **1996**, *383* (6601), 593−597.

(118) Curtis, M. E.; Sondergeld, C. H.; Ambrose, R. J.; Rai, C. S. Microstructural investigation of gas shales in two and three dimensions using nanometer-scale resolution imagingMicrostructure of Gas Shales. *AAPG Bull.* **2012**, *96* (4), 665−677.

(119) Peng, S.; Xiao, X. Investigation of multiphase fluid imbibition in shale through synchrotron-based dynamic micro-CT imaging. *Journal of Geophysical Research: Solid Earth* **2017**, *122* (6), 4475−4491.

(120) Loucks, R. G.; Reed, R. M.; Ruppel, S. C.; Jarvie, D. M. Morphology, genesis, and distribution of nanometer-scale pores in siliceous mudstones of the Mississippian Barnett Shale. *J. Sediment. Res.* **2009**, *79* (12), 848−861.

(121) Yassin, M. R.; Dehghanpour, H.; Begum, M.; Dunn, L. Evaluation of Imbibition Oil Recovery in the Duvernay Formation. *SPE Reservoir Eval. Eng.* **2018**, *21* (02), 257−272.

(122) Arif, M.; Barifcani, A.; Lebedev, M.; Iglauer, S. In CO_2 Wettability of Shales and Coals as a Function of Pressure, Temperature and Rank: Implications for CO_2 Sequestration and Enhanced Methane Recovery. In *PAPG/SPE Pakistan Section Annual Technical Conference and Exhibition*; Society of Petroleum Engineers, Islamabad, Pakistan, 2016.

(123) Loucks, R. G.; Reed, R. M.; Ruppel, S. C.; Hammes, U. Spectrum of pore types and networks in mudrocks and a descriptive classification for matrix-related mudrock pores. *AAPG Bull.* **2012**, *96* (6), 1071−1098.

(124) Nelson, P. H. Pore-throat sizes in sandstones, tight sandstones, and shales. *AAPG Bull.* **2009**, *93* (3), 329−340.

(125) Ougier-Simonin, A.; Renard, F.; Boehm, C.; Vidal-Gilbert, S. Microfracturing and microporosity in shales. *Earth-Sci. Rev.* **2016**, *162*, 198−226.

(126) Pan, B.; Yin, X.; Iglauer, S. A review on clay wettability: From experimental investigations to molecular dynamics simulations. *Adv. Colloid Interface Sci.* **2020**, *285*, 102266.

(127) Xu, M.; Dehghanpour, H. Advances in understanding wettability of gas shales. *Energy Fuels* **2014**, *28* (7), 4362−4375.

(128) Borysenko, A.; Clennell, B.; Sedev, R.; Burgar, I.; Ralston, J.; Raven, M.; Dewhurst, D.; Liu, K. Experimental investigations of the wettability of clays and shales. *J. Geophys. Res.* **2009**, *114* (B7), na.

(129) Liang, Y.; Tsuji, S.; Jia, J.; Tsuji, T.; Matsuoka, T. Modeling CO2−water−mineral wettability and mineralization for carbon geo-sequestration. *Acc. Chem. Res.* **2017**, *50* (7), 1530−1540.

(130) Chen, C.; Dong, B.; Zhang, N.; Li, W.; Song, Y. Pressure and temperature dependence of contact angles for CO2/water/silica systems predicted by molecular dynamics simulations. *Energy Fuels* **2016**, *30* (6), 5027−5034.

(131) Yu, X.; Li, J.; Chen, Z.; Wu, K.; Zhang, L.; Hui, G.; Yang, M. Molecular dynamics computations of brine-CO2/CH4-shale contact angles: Implications for CO2 sequestration and enhanced gas recovery. *Fuel* **2020**, *280*, 118590.

(132) Lin, K.; Yuan, Q.; Zhao, Y.-P. Using graphene to simplify the adsorption of methane on shale in MD simulations. *Comput. Mater. Sci.* **2017**, *133*, 99−107.

(133) Ren, Q.-Y.; Chen, G.-J.; Yan, W.; Guo, T.-M. Interfacial tension of (CO2+ CH4)+ water from 298 to 373 K and pressures up to 30 MPa. *J. Chem. Eng. Data* **2000**, *45* (4), 610−612.

(134) Liu, Y.; Li, H. A.; Okuno, R. Measurements and modeling of interfacial tension for CO2/CH4/brine systems under reservoir conditions. *Ind. Eng. Chem. Res.* **2016**, *55* (48), 12358−12375.

(135) Mosher, K.; He, J.; Liu, Y.; Rupp, E.; Wilcox, J. Molecular simulation of methane adsorption in micro-and mesoporous carbons with applications to coal and gas shale systems. *Int. J. Coal Geol.* **2013**, *109*, 36−44.

(136) Vandenbroucke, M.; Largeau, C. Kerogen origin, evolution and structure. *Org. Geochem.* **2007**, *38* (5), 719−833.

(137) Jagadisan, A.; Heidari, Z. Experimental Quantification of the Effect of Thermal Maturity of Kerogen on Its Wettability. *SPE Reservoir Eval. Eng.* **2019**, *22* (04), 1323−1333.

(138) Yang, R.; He, S.; Hu, Q.; Zhai, G.; Yi, J.; Zhang, L. Comparative investigations on wettability of typical marine, continental, and transitional shales in the middle Yangtze Platform (China). *Energy Fuels* **2018**, *32* (12), 12187−12197.

(139) Gensterblum, Y.; Busch, A.; Krooss, B. M. Molecular concept and experimental evidence of competitive adsorption of H_2O, CO_2 and CH_4 on organic material. *Fuel* **2014**, *115*, 581−588.

(140) Chareonsuppanimit, P.; Mohammad, S. A.; Robinson, R. L., Jr; Gasem, K. A. High-pressure adsorption of gases on shales: Measurements and modeling. *Int. J. Coal Geol.* **2012**, *95*, 34−46.

(141) Ju, Y.; He, J.; Chang, E.; Zheng, L. Quantification of CH_4 adsorption capacity in kerogen-rich reservoir shales: An experimental investigation and molecular dynamic simulation. *Energy* **2019**, *170*, 411−422.